Design, Synthesis and Biological Evaluation of Heterocycles for Tuberculosis

M.Sc. Thesis

By

Antim Rani

DEPARTMENT OF CHEMISTRY

INDIAN INSTITUTE OF TECHNOLOGY INDORE

May 2022

Design, Synthesis and Biological Evaluation of Heterocycles for Tuberculosis

A THESIS

Submitted in partial fulfilment of the requirements

for the award of the degree

of

Master of Science

by

Antim Rani

DEPARTMENT OF CHEMISTRY

INDIAN INSTITUTE OF TECHNOLOGY INDORE

May 2022

INDIAN INSTITUTE OF TECHNOLOGY INDORE

CANDIDATE'S DECLARATION

I hereby declare that the work which is being presented in the thesis entitled **Design, Synthesis and Biological Evaluation of Heterocycles for Tuberculosis** in the partial fulfilment of the requirements for the award of the degree of **MASTER OF SCIENCE** and submitted in the **DEPARTMENT OF CHEMISTRY, Indian Institute of Technology Indore**, is an authentic record of my own work carried out during the time period from August 2021 of joining the M.Sc. program to May 2022 of M.Sc. Thesis submission under the supervision of **Dr. Venkatesh Chelvam**, Department of Chemistry, IIT Indore.

The matter presented in this thesis has not been submitted by me for the award of any other degree of this or any other institute.

Antim Rani

Antim Rani

This is to certify that the above statement made by the candidate is correct to the best of my knowledge.

Venkatesh C

Dr. Venkatesh Chelvam

25.05.2022

Antim Rani has successfully given her M.Sc. Oral Examination held on **<Date of M.Sc. Oral Examination>**.

Venkatesh C

Signature of Supervisor of M.Sc. thesis

Date: 25.05.2022

Tushar Kanti Mukherjee

Convener, DPGC

Date: 27.05.2022

Signature of PSPC Member #1

Date: 27.05.2022

S. Sahoo

Signature of PSPC Member #2

Date: 27.05.2022

ACKNOWLEDGEMENTS

I want to express my deepest gratitude to my supervisor **Dr. Venkatesh Chelvam**, for giving me this exemplary opportunity to pursue research and for believing in my research abilities. His constant guidance, support, and encouragement have been extremely helpful. His enthusiasm and dedication to research have always inspired me. Further, I'd like to thank my PSPC members Prof. Sanjay K. Singh and Dr. Selvakumar Sermadurai for their valuable suggestions and support.

With great pleasure, I express my deep respect to the Director, IIT Indore, and the Dean of Academic Affairs (DOAA) for providing the research facilities, conferences, seminars, and workshops for an enriching research environment at the Indian Institute of Technology Indore. I'd also like to acknowledge Prof. Biswarup Pathak (Head, Department of Chemistry), and Dr. Tushar Kanti Mukherjee (DPGC Convener) for their suggestions and guidance in various aspects. I am also grateful to the Department of chemistry for their guidance and help during various activities**.**

I extend my profound thanks to my group members Dr. Mena Asha Krishnan, Ms. Kratika Yadav, Mr. Lekhnath Sharma, Mr. Tapash Kalita, Mr. Soumit Dutta and Mr. Saroj Ali for their generous cooperation, encouragement, and support.

Antim Rani

M.Sc. Student

DEDICATED TO MY FAMILY AND FRIENDS……

For their support in every stage of my life!

ABSTRACT

Tuberculosis (TB) is an infectious disease caused by the bacterium *Mycobacterium tuberculosis*. Currently, finding a cure to such a deadly disease is a matter of concern. Both multi-drug resistant TB and extremely drug-resistant TB are threats to success in the anti-TB programs. A rapid increase in cases of the resistance strains introduced an urgent requirement to develop new chemical compounds with improved efficacy. Azaindole is a promising core for anti-TB agents. Azaindoles have become an integral core moiety in the critical drug candidates. The present thesis work describes the synthesis and characterization of pyrrolopyridine-isatin hybrids. These hybrids serve as competitive inhibitors of polyketide synthetase 13 (Pks13), inhibiting mycolic acid synthesis. Moreover, these molecules can be further examined in the treatment of tuberculosis.

TABLE OF CONTENTS

LIST OF FIGURES

LIST OF SCHEMES

SYMBOLS/ UNITS

J	Coupling constant
δ	Delta
h	Hour
Hz/MHz	Hertz/Mega Hertz
mg	Milli gram
mL	Milliliter
R_f	Retardation factor
ppm	Parts per million

ACRONYMES

NH_4Cl	Ammonium chloride
BDQ	Bedaquiline
Bn	Benzyl
CaH_2	Calcium hydride
$CDCl_3$	Chloroform-d
d	Doublet
DCM	Dichloromethane
dd	Doublet of doublet
DIPEA	Diisopropylethyl amine
DLM	Delamanid
DMF	N,N-Dimethyl formamide
Et	Ethyl
EtOAc	Ethyl acetate
XDR-TB	Extremely drug-resistant tuberculosis
HCl	Hydrochloric acid
INH	Isoniazid
$LiAlH_4$	Lithium aluminium hydride
m	Multiplet
m.p.	Melting point
MDR-TB	Multidrug-resistant tuberculosis
M*tb*	*Mycobacterium tuberculosis*
NAD	Nicotinamide adenine dinucleotide
NMR	Nuclear magnetic resonance
K_2CO_3	Potassium carbonate
KOH	Potassium hydroxide
q	Quartet
RMP	Rifampin
s	Singlet
NaOAc	Sodium acetate

NaH	Sodium hydride
Na_2SO_4	Sodium sulphate
TB	Tuberculosis
THF	Tetrahydrofuran
TLC	Thin layer chromatography
TMS	Tetramethylsilane

Chapter 1

INTRODUCTION

1.1 Statistics of tuberculosis across the world and in India

Tuberculosis (TB) is the 13th leading cause of death by *Mycobacterium tuberculosis*, a contagious agent. In the year 2020, it was the second foremost infectious killer after COVID-19 (above HIV/AIDS). The most evident impact of COVID-19 pandemic is a large global drop in the number of newly diagnosed TB cases. India recorded 41% of the global decline (18% decline from 2019 to 2020) in TB cases. Because of the substantial global decline in newly diagnosed TB cases, there has been an increase in TB mortality. In the year 2020, 1.5 million deaths were reported from TB globally (including 2,14,000 people with HIV) and 34% of the global TB deaths were accounted for in India *[1]*.

Tuberculosis is a contagious infection caused by the bacterium called *Mycobacterium tuberculosis*. It generally affects the lungs and spreads to different parts of the body such as the kidney, brain, and spine. TB is broadly classified into two forms, active and latent, according to the symptoms or modes of action. MDR-TB is caused due to resistance for the TB drugs such as isoniazid (INH) and rifampicin (RMP). Only about one in three people with drug-resistant TB accessed treatment in 2020. Hence, efficient drug design and discovery are urgently required.

1.2 Treatment of tuberculosis

TB diseases are treatable and curable. TB treatment involves the use of antibiotics for killing the bacteria. Effective treatment for TB is difficult, due to the abnormal chemical composition and structure of the mycobacterial cell wall of M*tb*, which makes many antibiotics ineffective by hindering the entry of drugs. Treatment of active drug-susceptible TB

involves a dose combination of three or four drugs (INH, RMP, pyrazinamide, and ethambutol) for 6-12 months. Second-line TB remedies are utilized in the treatment of MDR-TB and need extensive chemotherapy treatment. These are limited, costly, as well as toxic. Bedaquiline (BDQ) and delamanid (DLM) are the only FDA-approved two recent new drugs for treating MDR-TB.

1.3 N-Heterocyclic compounds for drug development

Nitrogen-containing heterocyclic compounds are the most privileged category of organic compounds. Most of the drugs which are approved by the FDA and are available on the market contain N-heterocyclic moieties. These are present in the core of a wide range of biomolecules such as nucleic acids, amino acids, vitamins and carbohydrates, and alkaloids. N-heterocyclic compounds which are widely distributed in nature are the components of various biologically important molecules, such as vitamins, pharmaceuticals, nucleic acids, dyes, and antibiotics. The scope of drug development has been broadened due to the exceptional role of nitrogen in various interactions with biological targets.

1.3.1 Pyrrolopyridines

Pyrrolopyridines or azaindoles are the privileged structures and bioisosteres of the indole core *[2]*. These are an integral part of various drug-like molecules and several kinase inhibitors *[3]*. Azaindole derivatives exhibit promising anti-cancer activities *[4]*.

Azaindoles are natural variolin derivatives with cyclin-dependent kinase (CDK) inhibiting properties *[5, 6]*. Azaindole derivatives are well exploited in drug design and discovery as their properties could be modulated by varying the position of endocyclic nitrogen *[3]*. For preparing azaindoles the common synthetic strategies generally start with aminopyridines, then building up a pyrrole ring. Several methods for the synthesis of azaindoles are reviewed in the literature. Azaindoles

synthesized from aminopyridines involve Pd-catalyzed coupling reactions *[7]*, such as Heck *[8, 9]*, Sonogashira *[10]*, and Suzuki *[11]* couplings. Aminopyridines are the challenging precursors in metal catalysis *[12]*. The 5-azaindole isomer is widely encountered because of its strong similarity with 5-hydroxy indole which is an important metabolite of indole moiety present in various biomolecules, such as serotonin, and melatonin *[13]*. Azaindoles and methods for their synthesis have attracted the interest of scientists because of their physiochemical *[14]* and pharmacological properties *[15]* with various uses in the field of medicinal chemistry *[16, 17]*.

1.3.2 Furopyridines

In the past few decades, furopyridine moieties have been studied widely and attracted a tremendous amount of attention from the scientific community for their antituberculosis activity. Furopyridines are the isosteres of benzofuropyridine which have critical biological applications as M*tb* polyketide synthase 13 (Pks13) inhibitors *[18]*. These are identified as selective bioactive compounds against different strains of M*tb* which are drug-resistant. Furopyridine not only has a π-electron rich furan ring but also has a π-electron deficient pyridine ring. Due to this, such fused heterocycles show unique and interesting properties. Furopyridines are also found as polyketide synthase 13 (Pks13) inhibitors to control mycolic acid synthesis in *Mycobacterium tuberculosis [19]*. TAM16 is the most potent benzofuran-5-ol framework, *Mycobacterium tuberculosis* polyketide synthase 13 (Pks13) inhibitor which showed therapeutic potential in MDR-TB strains and is structurally very close to furo[3,2-c]pyridine *[20]*.

1.4 Mycolic acids and polyketide synthase (Pks) enzyme

The rapid increase in drug resistance of M*tb* is mainly due to the complex structure of its bacterial cell wall. The outermost layer of the

bacterial cell wall in M*tb* is made up of complex fatty acids called mycolic acid. The mycolic acid layer makes a hydrophobic protective layer around the bacterium and is important for virulence *[20]*. In M*tb*, more than 20 enzymes make a variety of multi-enzyme complexes for the biosynthesis of mycolic acid *[21]*. Most of the mycolic acid derivatives form mycolate-containing lipids, which play a critical role in pathologies caused by mycobacterium, acting either as pro-inflammatory agents or as T cell activators. Anti-TB agents disrupt various biosynthetic pathways for the formation of mycolic acid. Polyketide synthase 13 (Pks13) is an important key enzyme for the biosynthesis of mycolic acid. Recently it has emerged as a novel drug target for the treatment of MDR-TB and XDR-TB *[20]*. The biosynthetic pathway for MA is a validated target for many first-line and second-line anti-TB drugs. For instance, isoniazid (INH) pro-drug interactions with NAD (nicotinamide adenine dinucleotide) inhibit enoyl-ACP reductase, an important enzyme in MA synthesis. This was a key strategy against Mtb for several decades. Loss of mutations in the *inh*A gene and its promoter (KatG) region has rendered conventional drugs INH and ethionamide (ETH) ineffective *[22]*. Therefore, discovering a new category of molecules having anti-TB activity is an urgent need to set up a new standard treatment regimen for the complete eradication of this deadly disease.

1.5 Isatin hybrids

Isatin is an organic molecule found in many species *[23]* that has attracted a lot of attention in medicinal chemistry due to its biological properties, including anti-tuberculosis *[24]*, anti-bacterial *[25]*, and anti-tumor activities. Furthermore, research on isatin analogue structure-activity relationships revealed that 5-halogenation and N-alkylation were beneficial in boosting inhibitory activity against a variety of fungi, bacteria, and viruses *[26]*. As a result, isatin is a viable candidate for developing new anti-tuberculosis drugs.

Azole is an important class of nitrogen-containing heterocycles, which possess a variety of biological activities. The 1,2,3-triazole and its derivatives, which are easily synthesized by 'Click chemistry,' have attracted intellectual concerns. Indeed, the use of 'Click chemistry' has become one of the most popular methods for introducing structural variety in drug design. *[27]*. The excellent biological activities of 1,2,3-triazole rings are due to their advantageous features such as modest dipole character, hydrogen bonding ability, and persistence under *in vivo* conditions *[28]*.

The molecular hybridization concept, which is focused on merging the pharmacophore moieties of multiple bioactive substances to form a unique hybrid compound with enhanced affinity and efficacy relative to parent pharmaceuticals, is a recent concept in drug design *[29]*.

The anti-TB activity of several fluoroquinolone-isatin hybrids with various linkers such as methylene, ethylene, acetyl, and 1,2,3-triazole has been investigated *[30-35]*. According to the structure-activity relationship (SAR), the linkers between fluoroquinolones and isatin have a significant impact on the anti-TB activity of such hybrids. In general, the linkers have the following effects on anti-TB activity: 1,2,3-triazole > methylene > ethylene > acetyl.

In this study, we designed and synthesized pyrrolo[3,2-c]pyridine-isatin derivatives, which were inspired by the research carried out in our research group.

1.6 Objectives of the project

The major objectives of this project are to design and synthesize anti-TB drugs which will act as a competitive inhibitor of polyketide synthase 13 (Pks13) resulting in inhibition of biosynthesis of the mycolic acids and further evaluate their activities to improve MDR and XDR tuberculosis therapies.

Chapter 2

LITERATURE REVIEW

2.1 Synthesis of azaindoles

Pires *et al*. synthesized 2,3-disubstituted azaindoles **3** via a Pd-catalyzed one-pot C–N coupling of the alkenyl bromides **2** and o-aminobromopyridines **1** through one-step methodology *[36]*. The scope of the reaction is broad (Scheme 1).

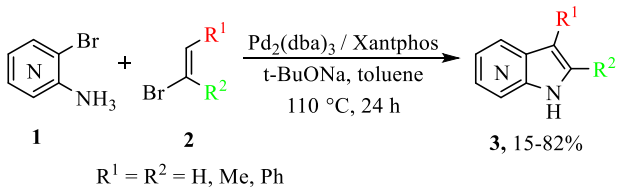

Scheme 1. Pd-catalyzed one-pot C–N cross-coupling or heck reaction

Calvet *et al.* synthesized substituted 5-azaindoles **5** via the Pd catalyzed hetero-annulation of 3-iodo-4-acetamidopyridines **4** and *p*-substituted diarylalkynes *[37]*. This reaction gives 2,3-diaryl-5-azaindoles **5** in high yields (Scheme 2).

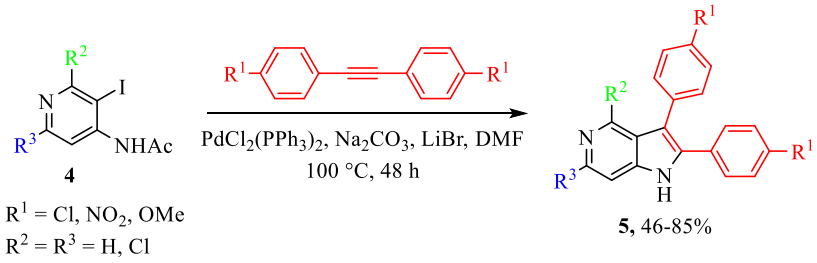

Scheme 2. Palladium-catalyzed hetero-annulation reaction of 2- or 6-chloro-4-acetamido-3-iodopyridines **4** with *p*-substituted diaryl alkynes

Purificação *et al*. synthesized 1,2-disubstituted 4-, 5-, 6-, and 7-azaindoles **7** from o-aminobromopyridines **6** via Pd catalyzed N-arylation followed by the Sonogashira coupling reaction and subsequent cyclization

in a one-pot manner *[38]*. This procedure gives 22-68% yields and has a wide substrate scope congruity with the electron-accepting and the electron-releasing groups (Scheme 3).

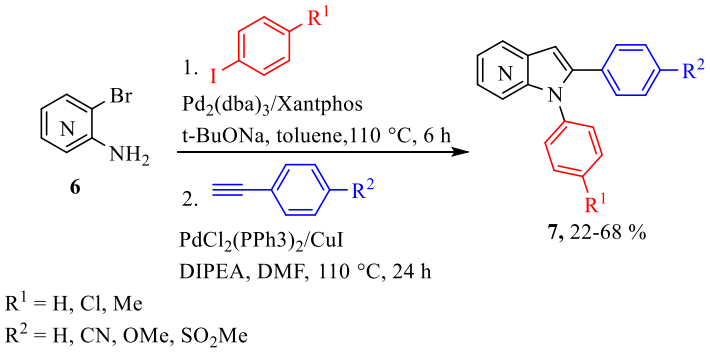

Scheme 3. Palladium-catalyzed one-pot synthetic route of 4-, 5-, 6-, and 7- azaindoles **7**

2.2 Synthesis of isatin hybrids

Sriram *et al*. *[30,39-40]* synthesized three fluoroquinolone methylene isatin hybrids, norfloxacin, ciprofloxacin, and gatifloxacin, and evaluated their anti-tuberculosis activity utilizing the molecular hybridization drug design method. The findings suggested that the newly established hybrids are effective against MTB.

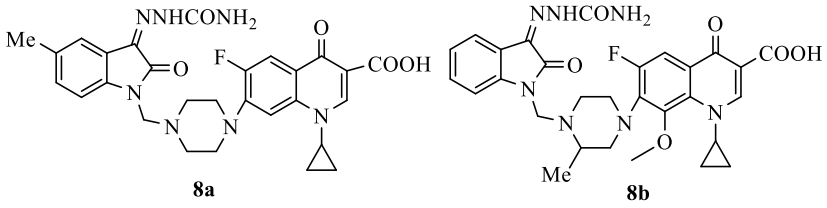

Figure 1. Ciprofloxacin methylene isatin-hybrid **8a** and gatifloxacin methylene isatin-hybrid **8b**

Dighe *et al*. *[41]* designed and evaluated two series of isatin-thiazole hybrids, azetidinone, and thiazolidinone derivatives, for anti-TB efficacy. The structure-activity correlation indicated that halogen compounds were more efficient than others.

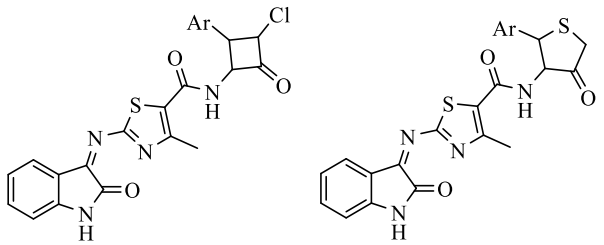

Figure 2. Isatin-thiazole azetidinone **9a** and thiazolidinone **9b** hybrids

Eldehna *et al. [42]* studied the effect of isatin moiety substitution at the C-5 position in hydrazides. It has moderate anti-tuberculosis action with an unsubstituted isatin moiety, according to the findings. Increased activity was achieved by adding a chlorine atom to the C-5 position. The addition of a bromine substituent significantly increased efficacy against MTB.

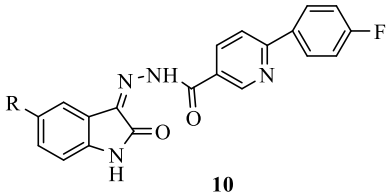

Figure 3. Isoniazide-isatin hybrids **10a-c**

Gao *et al*. recently synthesized benzofuran-isatin hybrid series against MTB H37Rv and MDR-TB strains *[43]*, which displayed significant *in vitro* anti-mycobacterial activity against both vulnerable and multidrug resistance M*tb* strains. In this situation, combining TAM16 with isatin resulted in novel hybrids with enhanced anti-TB efficacy than individual components.

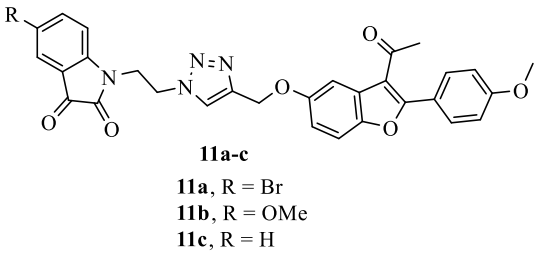

11a-c

11a, R = Br
11b, R = OMe
11c, R = H

Figure 4. Benzofuran-isatin hybrids **11a-c**

Chapter 3

EXPERIMENTAL SECTION

3.1 General information and methods

The moisture-sensitive reactions were performed using oven-dried glassware in a dry solvent under an inert environment. For transferring all moisture-sensitive liquids glass syringes were used under a nitrogen atmosphere. Under a nitrogen atmosphere, air and moisture-sensitive materials were also carefully transferred. The reaction was monitored using analytical TLC (thin layer chromatography) on Merck silica gel plates. TLC plates were analyzed using UV irradiation at 254 nm. UV inactive compounds were analyzed by staining with iodine or ninhydrin. The compounds were concentrated by evaporating the volatile solvents at 40 °C using a rotary evaporator under reduced pressure. All compounds were isolated through column chromatography. Distilled solvents were used as eluents for purifying the compounds through column chromatography. The Bruker AV 500 MHz NMR spectrometer was used to obtain NMR spectra. $CDCl_3$ was used as a solvent for preparing the NMR samples. Chemical shifts (δ) were measured in ppm (parts per million) using TMS as an internal reference. The Bruker Daltonik High Performance LC-MS (ESI-TOF) spectrometer was used to obtain high-resolution mass spectra.

3.2 Drying of solvents

For drying organic solvents, drying agents such as CaH_2 and anhydrous Na_2SO_4 were used.

3.2.1 Drying of THF/diethyl ether (Et_2O)

In a round bottom flask, the required amount of THF/diethyl ether was taken. Sodium wire and a pinch of benzophenone were added to it and refluxed till the solvent turned deep blue in color. The solvent was

distilled off and collected in another round bottom flask containing flame-dried 4Å molecular sieves.

3.2.2 Drying of DCM/ ACN/ toluene

In a round bottom flask, the required amount of DCM/ACN/toluene was taken. A pinch of CaH_2 was added to it and stirred overnight. The solvent was distilled off and collected in another round bottom flask containing flame-dried 4Å molecular sieves.

3.2.3 Drying of DMF

In a round bottom flask, the required amount of DMF was taken. A pinch of CaH_2 was added to it and stirred overnight. The solvent was distilled off by vacuum distillation and collected in another round bottom flask containing flame-dried 4Å molecular sieves.

3.3 Synthesis of starting materials

3.3.1 Synthesis of 1-methyl-1H-pyrrole-2-carbaldehyde (13a)

Diethyl ether (10 mL) was taken in a round bottom flask (50 mL). 18-crown-6 ether (0.16 mL, 0.73 mmol) and potassium tertiary butoxide (1.19 g, 10.52 mmol) were added at room temperature. Pyrrole-2-carbaldehyde (1.00 g, 10.52 mmol) was added to the reaction mixture in one portion and stirred for 15 minutes at the same temperature. At 0 °C, methyl iodide (0.65 mL, 10.52 mmol) was added dropwise using a glass syringe over a time of 5 minutes. The reaction mixture was brought to room temperature, stirred for 24 hours, and monitored by TLC. After the completion of the reaction, the mixture was diluted with milli-Q water (MQ, 5 mL) and with EtOAc (5 mL), followed by extraction of the aqueous layer with EtOAc (3 × 5 mL). Then, the organic layer was washed with brine (5 mL), dried over anhydrous Na_2SO_4, filtered, and concentrated to obtain the crude residue. The crude residue was purified through column chromatography over silica gel (230-400 mesh) to afford

13a. **Yield** 70% (0.95 g); Light yellow liquid; $\mathbf{R_f}$ 0.4 (4:1 hexane-EtOAc); **^{1}H NMR** (400 MHz, $CDCl_3$) δ 9.54 (s, 1H), 6.98–6.88 (m, 1H), 6.88–6.83 (m, 1H), 6.25–6.17 (m, 1H), 3.95 (s, 3H**)**; **^{13}C NMR** (100 MHz, $CDCl_3$) δ 179.6, 132.1, 132.0, 124.1, 109.5, 36.5.

3.3.2 Synthesis of 1-benzyl-1H-pyrrole-2-carbaldehyde (13b)

Dimethyl sulfoxide (10 mL) was taken in a single-neck round-bottom flask (100 mL). Crushed potassium hydroxide (1.18 g, 21 mmol) was added and stirred for 5 minutes at room temperature. Pyrrole-2-carbaldehyde (0.50 g, 5.25 mmol) was added to the reaction mixture in one portion and stirred for 45 minutes at the same temperature. At 0 °C, benzyl bromide (1.25 mL, 10.5 mmol) was added dropwise using a glass syringe over a period of 5 minutes. The reaction mixture was brought to room temperature, stirred for 45 minutes, and monitored by TLC. After the completion of the reaction, the mixture was diluted with milli-Q water (MQ, 5 mL) and with DCM (5 mL), followed by extraction of the aqueous layer with DCM (4 × 10 mL). The organic layer was washed with brine (5 mL), dried over anhydrous Na_2SO_4, filtered, and concentrated to obtain the crude residue. The crude residue was purified through column chromatography over silica gel (230-400 mesh) to afford **13b**. **Yield** 75% (0.82 g); Yellow oily liquid; $\mathbf{R_f}$ 0.4 (9:1 hexane-EtOAc); **^{1}H NMR** (400 MHz, $CDCl_3$) δ 9.47 (s, 1H), 7.27–7.13 (m, 3H), 7.12–7.00 (m, 2H), 6.93–6.80 (m, 2H), 6.18 (dd, J = 3.2, 2.7 Hz, 1H), 5.47 (s, 2H); **^{13}C NMR** (100 MHz, $CDCl_3$) δ 179.5, 137.6, 131.6, 131.4, 128.7, 127.7, 127.3, 124.8, 110.2, 52.0.

3.3.3 Synthesis of 1-(4-methoxybenzyl)-1H-pyrrole-2-carbaldehyde (13c)

NaH (60% suspension in mineral oil, 0.10 g, 2.52 mmol) was taken in a two-neck round-bottom flask (50 mL). Dry DMF (3 mL) was added under an inert atmosphere at room temperature. Pyrrole-2-carbaldehyde

(0.20 g, 2.10 mmol) was added to the reaction mixture in one portion and stirred for 30 minutes at the same temperature. At 0 °C, 4-methoxy benzyl chloride (0.34 mL, 2.52 mmol) was added dropwise using a glass syringe over a period of 5 minutes under an inert atmosphere. The reaction mixture was warmed to room temperature, stirred for 2 hours, and monitored by TLC. After the completion of the reaction, the mixture was diluted with milli-Q water (MQ, 10 mL) and with DCM (5 mL), followed by extraction of the aqueous layer with DCM (3 × 5 mL). The organic layer was washed with brine (5 mL), dried over anhydrous Na_2SO_4, filtered, and concentrated under reduced pressure to obtain the crude residue. The crude residue was purified over silica gel (230-400 mesh) column chromatography to 0obtain **13c**. **Yield** 80% (0.43 g); Dark yellow oily liquid; $\mathbf{R_f}$ 0.45 (4:1 hexane-EtOAc); **^{1}H NMR** (400 MHz, $CDCl_3$) δ 9.55 (s, 1H), 7.13 (d, J = 8.3 Hz, 2H), 6.98–6.91 (m, 2H), 6.83 (d, J = 8.3 Hz, 2H), 6.24 (dd, J = 2.8, 2.4 Hz, 1H), 5.48 (s, 2H), 3.76 (s, 3H); **^{13}C NMR** (100 MHz, $CDCl_3$) δ 179.5, 159.2, 131.5, 131.2, 129.6, 128.9, 124.9, 114.1, 110.1, 55.3, 51.5.

3.4 Synthesis of alkyl 4-(1H-pyrrol-2-yl)-1H-pyrrolo[3,2-c]pyridine-6-carboxylate derivatives

3.4.1 Synthesis of methyl1-methyl-4-(1-methyl-1H-pyrrol-2-yl)-1H-pyrrolo[3,2-c]pyridine-6-carboxylate (14a)

Glycine methyl ester hydrochloride (0.17 g, 1.37 mmol), N-methyl pyrrole-2-aldehyde (0.30 g, 2.75 mmol) and DIPEA (0.96 mL, 5.50 mmol) were heated in a sealed tube at 150 °C for 7 hours with constant stirring. The reaction mixture was brought to room temperature and diluted with milli-Q water (MQ, 10 mL) and EtOAc (5 mL), followed by extraction of the aqueous layer with EtOAc (3 × 5 mL). The organic layer was washed with brine (5 mL), dried over anhydrous Na_2SO_4, filtered, and concentrated to obtain the crude residue. The crude residue was purified over alumina (neutral, 100 mesh) column chromatography to obtain **14a**.

Yield 48% (0.18 g); Yellowish-brown solid; **m.p.** = 120–122 °C; $\mathbf{R_f}$ 0.42 (1:1 hexane-EtOAc); **^{1}H NMR** (500 MHz, $CDCl_3$) δ 8.03 (s, 1H), 7.18 (d, J = 3.0 Hz, 1H), 6.83 (d, J = 3.5 Hz, 1H), 6.78 (t, J = 2.5 Hz, 1H), 6.74 (m, 1H), 6.22 (t, J = 3.2 Hz, 1H), 4.06 (s, 3H), 3.99 (s, 3H), 3.79 (s, 3H); **^{13}C NMR** (125 MHz, $CDCl_3$) δ 167.3, 145.6, 140.6, 138.3, 131.8, 130.6, 126.1, 124.7, 112.5, 107.4, 105.3, 102.9, 52.4, 36.3, 32.9; **HRMS** (ESI) calcd for [$C_{15}H_{15}N_3O_2$+H^+] 270.1237, found 270.1237.

3.4.2 Synthesis of methyl1-ethyl-4-(1-ethyl-1H-pyrrol-2-yl)-1H-pyrrolo[3,2-c]pyridine-6-carboxylate (14b)

Glycine methyl ester hydrochloride (0.08 g, 0.65 mmol), N-ethyl pyrrole-2-aldehyde (0.20 g, 1.62 mmol) and DIPEA (0.39 mL, 2.27 mmol) were heated in a sealed tube at 135 °C for 40 hours with constant stirring. The reaction mixture was brought to room temperature and diluted with milli-Q water (MQ, 10 mL) and EtOAc (5 mL), followed by extraction of the aqueous layer with EtOAc (3 × 5 mL). The organic layer was washed with brine (5 mL), dried over anhydrous Na_2SO_4, filtered, and concentrated to obtain the crude residue. The crude residue was purified over silica gel (230-400 mesh) column chromatography to afford **14b**. **Yield** 18% (0.04 g); Yellowish-brown oily liquid; $\mathbf{R_f}$ 0.4 (7:3 hexane-EtOAc); **^{1}H NMR** (500 MHz, $CDCl_3$) δ 8.09 (s, 1H), 7.30 (d, J = 3 Hz, 1H), 6.90-6.87 (m, 2H), 6.74 (dd, J = 3.7, 1.7 Hz, 1H), 6.25 (m, 1H), 4.57 (q, J = 7.0 Hz, 2H), 4.26 (q, J = 7.5 Hz, 2H), 4.00 (s, 3H), 1.52 (t, J = 7.3 Hz, 3H), 1.37 (t, J = 7.0 Hz, 3H),; **^{13}C NMR** (125 MHz, $CDCl_3$) δ 167.4, 145.7, 139.7, 138.3, 130.1, 129.9, 124.8, 124.2, 112.6, 107.5, 105.3, 103.1, 52.3, 43.3, 41.2, 16.9, 15.6; **HRMS** (ESI) calcd for [$C_{17}H_{19}N_3O_2$+H^+] 298.1550, found 298.1555.

3.4.3 Synthesis of ethyl1-methyl-4-(1-methyl-1H-pyrrol-2-yl)-1H-pyrrolo[3,2-c]pyridine-6-carboxylate (14c)

Glycine ethyl ester hydrochloride (0.19 g, 1.38 mmol), N-methyl pyrrole-2-aldehyde (0.30 g, 2.75 mmol) and DIPEA (0.96 mL, 5.50 mmol) were heated in a sealed tube at 150 °C for 7 hours with constant stirring. The reaction mixture was brought to room temperature and diluted with milli-Q water (MQ, 10 mL) and EtOAc (5 mL), followed by extraction of the aqueous layer with EtOAc (3 × 5 mL). The organic layer was washed with brine (5 mL), dried over anhydrous Na_2SO_4, filtered, and concentrated to obtain the crude residue. The crude residue was purified over silica gel (230-400 mesh) column chromatography to afford **14c**. **Yield** 46% (0.07 mg); Grey solid; **m.p.** = 118–120 °C; $\mathbf{R_f}$ 0.34 (7:3 hexane-EtOAc); **^{1}H NMR** (400 MHz, $CDCl_3$) δ 8.05 (s, 1H), 7.24 (d, J = 3.5 Hz, 1H), 6.89–6.88 (m, 1H), 6.81 (t, J = 2.2 Hz, 1H), 6.78 (dd, J = 3.5, 1.7 Hz, 1H), 6.24–6.23 (m, 1H), 4.47 (q, J = 7.2 Hz, 2H), 4.11 (s, 3H), 3.89 (s, 3H), 1.46 (t, J = 7.2 Hz, 3H); **^{13}C NMR** (125 MHz, $CDCl_3$) δ 166.8, 145.4, 140.6, 138.6, 131.8, 130.6, 126.2, 124.5, 112.5, 107.4, 105.1, 102.9, 61.2, 36.5, 32.9, 14.3; **HRMS** (ESI) calcd for [$C_{16}H_{17}N_3O_2$+H^+] 284.1394, found 284.1394.

3.4.4 Synthesis of *tert*-butyl1-methyl-4-(1-methyl-1H-pyrrol-2-yl)-1H-pyrrolo[3,2-c]pyridine-6-carboxylate (14d)

Glycine *tert*-butyl ester hydrochloride (0.15 g, 0.92 mmol), N-methyl pyrrole-2-aldehyde (0.20 g, 1.83 mmol) and DIPEA (0.57 mL, 3.28 mmol) were heated in a sealed tube at 150 °C for 8 hours with constant stirring. The reaction mixture was brought to room temperature and diluted with milli-Q water (MQ, 10 mL) and EtOAc (5 mL), followed by extraction of the aqueous layer with EtOAc (3 × 5 mL). The organic layer was washed with brine (5 mL), dried over anhydrous Na_2SO_4, filtered, and concentrated to obtain the crude residue. The crude residue was purified over alumina (neutral, 100 mesh) column chromatography to afford **14d**. **Yield** 29% (0.08 g); Brownish-yellow solid; **m.p.** = 152–154 °C; $\mathbf{R_f}$ 0.45 (7:3 hexane-EtOAc); **^{1}H NMR** (500 MHz, $CDCl_3$) δ 7.97 (s,

1H), 7.20 (d, *J* = 3.5 Hz, 1H), 6.88 (d, *J* = 3.0 Hz, 1H), 6.80 (d, *J* = 3.0 Hz, 2H), 6.25–6.24 (t, *J* = 3.0 Hz, 1H), 4.16 (s, 3H), 3.85 (s, 3H), 1.67 (s, 9H); **^{13}C NMR** (125 MHz, $CDCl_3$) δ 165.8, 145.1, 140.7, 139.7, 131.5, 130.7, 126.1, 123.9, 112.4, 107.3, 104.5, 102.6, 80.8, 36.6, 32.8, 28.1; **HRMS** (ESI) calcd for [$C_{18}H_{21}N_3O_2$+H^+] 312.1707, found 312.1708.

3.5 Synthesis of (1-methyl-4-(1-methyl-1H-pyrrol-2-yl)-1H-pyrrolo[3,2-c]pyridin-6-yl)methanol (15)

In a two neck round bottom flask (50 mL), **14a** (0.10 g, 0.37 mmol) and dry THF (2 mL) were added under an inert atmosphere and stirred for 5 minutes at 0 °C. Solid $LiAlH_4$ (0.05 g, 1.30 mmol) was added in single portion and the mixture was brought to room temperature and further stirred for 10 hours. After the completion of reaction, the mixture was diluted with saturated NH_4Cl (10 mL) and EtOAc (10 mL), followed by extraction of the aqueous layer with EtOAc (10 × 3 mL). The organic layer was washed with brine (5 mL), dried over anhydrous Na_2SO_4, filtered, and concentrated to obtain the crude residue. The crude residue was purified over silica gel (100–200 mesh) column chromatography to afford **15**; **Yield** 84% (0.08 g); Brown gummy liquid; $\mathbf{R_f}$ 0.16 (1:1 hexane-EtOAc); **^{1}H NMR** (500 MHz, $CDCl_3$) δ 7.07 (d, *J* = 3.0 Hz, 1H), 7.04 (s, 1H), 6.81 (t, *J* = 2.2 Hz, 1H), 6.79–6.78 (m, 1H), 6.74 (dd, *J* = 3.7, 1.8 Hz, 1H), 6.28–6.27 (m, 1H), 4.87 (s, 2H), 3.97 (s, 3H), 3.76 (s, 3H); **^{13}C NMR** (125 MHz, $CDCl_3$) δ 149.6, 144.8, 141.9, 131.1, 129.9, 125.8, 122.5, 112.4, 107.8, 102.4, 98.8, 64.9, 36.5, 32.9.; **HRMS** (ESI) calcd for [$C_{14}H_{15}N_3O$+H^+] 242.1288, found 242.1288.

3.6 Synthesis of 1-methyl-4-(1-methyl-1H-pyrrol-2-yl)-6-((prop-2-yn-1-yloxy)methyl)-1H- pyrrolo[3,2-c]pyridine (16)

In a round bottom flask (25 mL), **15** (0.05 g, 0.21 mmol) and dry DMF (3 mL) were added under an inert atmosphere and stirred for 5 minutes at 0 °C. NaH (60% suspension in mineral oil, 0.02 g, 0.41 mmol)

was added in a single portion and the mixture was stirred for 20 minutes at the same temperature. Propargyl bromide (80% in toluene, 33 μL, 0.31 mmol) was added dropwise using a micropipette. Further, the mixture was brought to room temperature and stirred for 10 hours. After the completion of reaction, the mixture was diluted with brine (5 mL) and EtOAc (10 mL), followed by extraction of the aqueous layer with EtOAc (10 × 3 mL). The extracted organic layer was dried over anhydrous Na_2SO_4, filtered, and concentrated to obtain the crude residue that was purified over silica gel (100–200 mesh) column chromatography to afford **16**; **Yield** 74% (0.04 g); Yellow oily liquid; $\mathbf{R_f}$ 0.75 (3:2 hexane-EtOAc); **^{1}H NMR** (500 MHz, $CDCl_3$) δ 7.26 (s, 1H), 7.05 (d, J = 3.0 Hz, 1H), 6.78-6.76 (m, 2H), 6.71 (dd, J = 3.7, 1.7 Hz, 1H), 6.24–6.23 (m, 1H), 4.87 (s, 2H), 4.33 (d, J = 2 Hz, 2H), 3.98 (s, 3H), 3.79 (s, 3H), 2.48 (t, J = 2.3 Hz, 1H); **^{13}C NMR** (125 MHz, $CDCl_3$) δ 147.9, 145.4, 141.9, 129.8, 125.8, 122.3, 112.4, 107.7, 102.5, 100.5, 74.7, 73.4, 57.9, 36.4, 32.9, 29.8; **HRMS** (ESI) calcd for [$C_{14}H_{15}N_3O+H^+$] 280.1444, found 280.1444.

3.7 General procedure for the synthesis of bromo-isatin derivatives (18a-d)

In a two neck round bottom flask (100 mL), a suspension of K_2CO_3 [for **18a** (0.19 g, 13.59 mmol), for **18b** (0.08 g, 6.06 mmol), for **18c** (0.19 g, 13.96 mmol), for **18d** (0.07 g, 5.08 mmol)] was prepared in dry DMF (5–10 mL) at room temperature. Further, indoline-2,3-dione (2.00 g, 13.59 mmol), 5-fluoro-indoline-2,3-dione (0.50 g, 3.02 mmol), 5-methyl-indoline-2,3-dione (1.50 g, 9.31 mmol), and 5-methoxy-indoline-2,3-dione (0.60 g, 3.39 mmol) were added to the suspension respectively and the mixture was stirred for 20 minutes. 1,2-Dibromoethane [for **18a** (2.4 mL, 27.19 mmol), for **18b** (0.6 mL, 6.66 mmol), for **18c** (1.7 mL, 18.62 mmol), for **18d** (0.6 mL, 6.77 mmol)] was added dropwise, and the mixture was further stirred for 16–40 hours. After the completion of the reaction, the mixture was diluted with brine (10 mL) and EtOAc (10 mL),

followed by extraction of the aqueous layer with EtOAc (6 × 10 mL). The extracted organic layer was dried over anhydrous Na_2SO_4, filtered, and concentrated to obtain the crude residue. The crude residue was purified over silica gel (230–400 mesh) column chromatography to afford **18a-d**.

3.7.1 1-(2-Bromoethyl)indoline-2,3-dione (18a)

Yield 70% (2.34 g); Yellow orange solid; **m.p.** = 124–126 °C; $\mathbf{R_f}$ 0.57 (1:1 hexane-EtOAc); **^{1}H NMR** (500 MHz, $CDCl_3$) δ 7.62–7.59 (m, 2H), 7.13 (t, J = 7.5 Hz, 1H), 7.00 (d, J = 8.5 Hz, 1H), 4.14 (t, J = 6.8 Hz, 2H), 3.60 (t, J = 7.2 Hz, 2H); **^{13}C NMR** (125 MHz, $CDCl_3$) δ 182.8, 158.3, 150.5, 138.6, 125.8, 124.2, 117.7, 110.4, 42.0, 27.3; **HRMS** (ESI) calcd for $[C_{10}H_8BrNO_2+Na^+]$ 275.9631, found 275.9629.

3.7.2 1-(2-Bromoethyl)-5-fluoroindoline-2,3-dione (18b)

Yield 59% (0.49 g); Red orange solid; **m.p.** = 66–68 °C; $\mathbf{R_f}$ 0.66 (1:1 hexane-EtOAc); **^{1}H NMR** (500 MHz, $CDCl_3$) δ 7.33–7.24 (m, 2H), 7.02 (dd, J = 8.6, 3.5 Hz, 1H), 4.12 (t, J = 6.7 Hz, 2H), 3.59 (t, J = 6.5 Hz, 2H); **^{13}C NMR** (125 MHz, $CDCl_3$) δ 182.3, 160.3, 158.0, 146.6, 125.0, 118.2, 112.6, 111.7, 42.1, 27.4; **HRMS** (ESI) calcd for $[C_{10}H_7BrFNO_2+Na^+]$ 293.9536, found 293.9536.

3.7.3 1-(2-Bromoethyl)-5-methylindoline-2,3-dione (18c)

Yield 65% (1.60 g); Red solid; **m.p.** = 114–116 °C; $\mathbf{R_f}$ 0.68 (1:1 hexane-EtOAc); **^{1}H NMR** (500 MHz, $CDCl_3$) δ 7.40–7.38 (m, 2H), 6.88 (d, J = 8 Hz, 1H), 4.10 (t, J = 6.8 Hz, 2H), 3.58 (t, J = 6.7 Hz, 2H), 2.31 (s, 3H).; **^{13}C NMR** (125 MHz, CDC_{l3}) δ 183.3, 158.6, 148.5, 139.2, 134.2, 126.2, 117.8, 110.4, 42.2, 27.6, 20.9; **HRMS** (ESI) calcd for $[C_{11}H_{10}BrNO_2+Na^+]$ 289.9787, found 289.9789.

3.7.4 1-(2-Bromoethyl)-5-methoxyindoline-2,3-dione (18d)

Yield 70% (0.67 g); Blood red solid; **m.p.** = 132–134 °C; $\mathbf{R_f}$ 0.7 (1:1 hexane-EtOAc); **^{1}H NMR** (500 MHz, $CDCl_3$) δ 7.15–7.13 (m, 2H), 6.91 (d, J = 8.0 Hz, 1H), 4.10 (t, J = 6.5 Hz, 2H), 3.79 (s, 3H), 3.58 (t, J = 6.7 Hz, 2H); **^{13}C NMR** (125 MHz, $CDCl_3$) δ 183.4, 158.7, 157.0, 144.7, 125.2, 118.5, 111.7, 110.1, 56.4, 42.4, 27.6; **HRMS** (ESI) calcd for $[C_{11}H_{10}BrNO_3+Na^+]$ 305.9736, found 305.9737.

3.8 General procedure for the synthesis of azido-isatin derivatives (19a-d)

In a round bottom flask (100 mL) **18a-d** (0.10 g, 0.37 mmol) were dissolved in DMF (2–3 mL). Sodium azide (0.10 g, 1.57 mmol) was added in one portion, under an inert atmosphere at room temperature and the mixture was stirred for 12–16 hours. After the completion of the reaction, the mixture was diluted with brine (10 mL) and DCM (10 mL), followed by extraction of the aqueous layer with DCM (3 × 10 mL). The extracted organic layer was dried over anhydrous Na_2SO_4, filtered, and concentrated to obtain the crude residue. The crude residue was purified over silica gel (100–200 mesh) column chromatography to afford **19a-d**.

3.8.1 1-(2-Azidoethyl)indoline-2,3-dione (19a)

Yield 95% (0.08 g); Orange solid; **m.p.** = 70–72 °C; $\mathbf{R_f}$ 0.21 (7:3 hexane-EtOAc); **^{1}H NMR** (500 MHz, $CDCl_3$) δ 7.61–7.56 (m, 2H), 7.11 (t, J = 7.5 Hz, 1H), 7.01 (d, J = 8 Hz, 1H), 3.88 (t, J = 6 Hz, 2H), 3.64 (t, J = 6 Hz, 2H); **^{13}C NMR** (125 MHz, $CDCl_3$) δ 183.1, 158.7, 150.9, 138.9, 125.8, 124.3, 117.8, 110.7, 49.2, 39.9; **HRMS** (ESI) calcd for $[C_{10}H_8N_4O_2+Na^+]$ 239.0539, found 239.0539.

3.8.2 1-(2-Azidoethyl)-5-fluoroindoline-2,3-dione (19b)

Yield 93% (0.08 g); Red solid; **m.p.** = 72–74 °C; $\mathbf{R_f}$ 0.53 (1:1 hexane-EtOAc); **^{1}H NMR** (500 MHz, $CDCl_3$) δ 7.35–7.30 (m, 2H), 7.01 (dd, J = 8.5, 3.6 Hz, 1H), 3.88 (t, J = 5.7 Hz, 2H), 3.67 (t, J = 5.7 Hz, 2H);

^{13}C NMR (125 MHz, $CDCl_3$) δ 182.6, 160.71, 158.5, 147.1, 125.3, 118.6, 112.1, 49.5, 40.2; **HRMS** (ESI) calcd for [$C_{10}H_7FN_4O_2$+Na^+] 257.0445, found 257.0443.

3.8.3 1-(2-Azidoethyl)-5-methylindoline-2,3-dione (19c)

Yield 95% (0.08 g); Orange-red solid; **m.p.** = 84–86 °C; $\mathbf{R_f}$ 0.68 (1:1 hexane-EtOAc); **^{1}H NMR** (500 MHz, $CDCl_3$) δ 7.41–7.39 (m, 2H), 6.89 (d, J = 8.0 Hz, 1H), 3.86 (t, J = 6.0 Hz, 2H), 3.63 (t, J = 6.0 Hz, 2H), 2.32 (s, 3H); **^{13}C NMR** (125 MHz, $CDCl_3$) δ 183.4, 158.9, 148.8, 139.3, 134.2, 126.2, 117.9, 110.5, 49.3, 39.9, 20.9; **HRMS** (ESI) calcd for [$C_{11}H_{10}N_4O_2$+Na^+] 253.0696, found 253.0696.

3.8.4 Synthesis of 1-(2-azidoethyl)-5-methoxyindoline-2,3-dione (19d)

Yield 95% (0.08 g); Blood red solid; **m.p.** = 100–102 °C; $\mathbf{R_f}$ 0.56 (1:1 hexane-EtOAc); **^{1}H NMR** (500 MHz, $CDCl_3$) δ 7.16–7.12 (m, 2H), 6.93 (d, J = 8.5 Hz, 1H), 3.85 (t, J = 5.7 Hz, 2H), 3.79 (s, 3H), 3.64 (t, J = 5.7 Hz, 2H); **^{13}C NMR** (125 MHz, $CDCl_3$) δ 183.5, 158.9, 156.9, 144.9, 125.2, 118.4, 111.8, 110.0, 56.4, 49.5, 40.1; **HRMS** (ESI) calcd for [$C_{11}H_{10}N_4O_3$+Na^+] 269.0645, found 269.0643.

3.9 Synthesis of pyrrolo[3,2-c]pyridine-isatin hybrid

3.9.1 Synthesis of 1-(2-(4-(((1-methyl-4-(1-methyl-1H-pyrrol-2-yl)-1H-pyrrolo[3,2-c]pyridin-6-yl)methoxy)methyl)-1H-1,2,3-triazol-1-yl)ethyl)indoline-2,3-dione (20)

In a round bottom flask (10 mL), **16** (0.04 g, 0.13 mmol) and **19a** (0.03 g, 0.13 mmol) were dissolved in DMF (2 mL). Monohydrate copper acetate (0.01 g, 0.06 mmol) and sodium ascorbate (0.02 g, 0.10 mmol) were added in one portion, at room temperature under an inert atmosphere. The mixture was stirred for 16 hours. After the completion of reaction, the mixture was diluted with brine (10 mL) and EtOAc (10 mL), followed by extraction of the aqueous layer with EtOAc (5 × 5 mL). The extracted

organic layer was dried over anhydrous Na_2SO_4, filtered, and concentrated to obtain the crude residue. The crude residue was purified over alumina (neutral, 175 mesh) column chromatography to afford **20**; **Yield** 48% (0.03 g); Blood-red solid; **m.p.** = 76–78 °C; $\mathbf{R_f}$ 0.1 (1:4 hexane-EtOAc); **^{1}H NMR** (500 MHz, $CDCl_3$) δ 7.63 (s, 1H), 7.49–7.47 (m, 1H), 7.44–7.41 (m, 1H), 7.21 (s, 1H), 7.06 (d, J = 3 Hz, 1H), 6.96 (t, J = 7.5 Hz, 1H), 6.77–6.74 (m, 2H), 6.69 (dd, J = 3.7, 1.8 Hz, 1H), 6.58 (d, J = 8.0 Hz, 1H), 6.23–6.22 (m, 1H), 4.73 (d, J = 2.0 Hz, 4H), 4.67 (t, J = 6.0 Hz, 2H), 4.21 (t, J = 6.3 Hz, 2H), 3.94 (s, 3H), 3.79 (s, 3H); **^{13}C NMR** (125 MHz, $CDCl_3$) δ 182.6, 158.7, 150.2, 148.2, 145.9, 145.3, 141.9, 138.9, 131.3, 129.8, 125.8, 125.8, 124.3, 123.9, 122.3, 117.5, 112.3, 109.7, 107.7, 102.5, 100.5, 74.0, 63.9, 47.8, 40.8, 36.4, 33.0; **HRMS** (ESI) calcd for $[C_{27}H_{25}N_4O_3+H^+]$ 496.2092, found 496.2091.

3.9.2 Synthesis of 5-methyl-1-(2-(4-(((1-methyl-4-(1-methyl-1H-pyrrol-2-yl)-1H-pyrrolo[3,2-c]pyridin-6-yl)methoxy)methyl)-1H-1,2,3-triazol-1-yl)ethyl)indoline-2,3-dione (21)

In a round bottom flask (25 mL), **16** (0.07 g, 0.23 mmol) and **19c** (0.04 g, 0.16 mmol) were dissolved in DMF (2 mL). Monohydrate copper acetate (0.02 g, 0.08 mmol) and sodium ascorbate (0.03 g, 0.12 mmol) were added in one portion, at room temperature under an inert atmosphere. The mixture was stirred for 16 hours. After the completion of reaction, the mixture was diluted with brine (10 mL) and EtOAc (10 mL), followed by extraction of the aqueous layer with EtOAc (5 × 5 mL). The extracted organic layer was dried over anhydrous Na_2SO_4, filtered, and concentrated to obtain the crude residue. The crude residue was purified over alumina (neutral, 175 mesh) column chromatography to afford **21**; **Yield** 58% (0.05 g); Reddish-orange solid; $\mathbf{R_f}$ (1:4 hexane-EtOAc); **^{1}H NMR** (500 MHz, $CDCl_3$) δ 7.60 (s, 1H), 7.24–7.19 (m, 3H), 7.03 (d, J = 3.0 Hz, 1H), 6.74–6.71 (m, 2H), 6.66 (dd, J = 3.7, 1.8 Hz, 1H), 6.44 (d, J = 8.0 Hz, 1H), 6.20–6.19 (m, 1H), 4.71 (d, J = 4.0 Hz, 4H), 4.63 (t, J = 6.0 Hz, 2H),

4.15 (t, J = 6.0 Hz, 2H), 3.92 (s, 3H), 3.77 (s, 3H), 2.14 (s, 3H); **^{13}C NMR** (125 MHz, $CDCl_3$) δ 182.8, 158.7, 148.2, 147.9, 145.8, 145.3, 141.8, 139.2, 134.2, 131.3, 129.7, 126.0, 125.7, 123.9, 122.2, 117.5, 112.2, 109.5, 107.6, 102.4, 100.4, 74.0, 63.9, 47.7, 40.7, 36.4, 32.9, 20.6; **HRMS** (ESI) calcd for $[C_{27}H_{25}N_4O_3+H^+]$ 510.2248, found 510.2248.

Chapter 4

RESULTS AND DISCUSSION

4.1 Synthetic schemes

4.1.1 Synthetic route of 1-methyl-1H-pyrrole-2-carbaldehyde (13a), 1-benzyl-1H-pyrrole-2-carbaldehyde (13b), and 1-(4-methoxybenzyl)-1H-pyrrole-2-carbaldehyde (13c)

The synthesis of **13** begins with commercially available pyrrole-2-carbaldehyde. The presence of pyrrole acidic N-H proton in **12** may interfere during the multistep synthesis of our model substrate; hence it needs to be protected first. The NH group was methylated, benzylated or protected with 4-methoxybenzyl group using methyl iodide, benzyl bromide or 4-methoxy benzyl chloride in the presence of KO^{t}Bu, KOH or NaH respectively. The base deprotonates NH, making it a good nucleophile that attacks methyl iodide, benzyl bromide or 4-methoxy benzyl chloride in S_N^2 fashion to yield the N-methylated, N-benzylated or N-(4-methoxybenzyl) derivative **13** (Scheme 4).

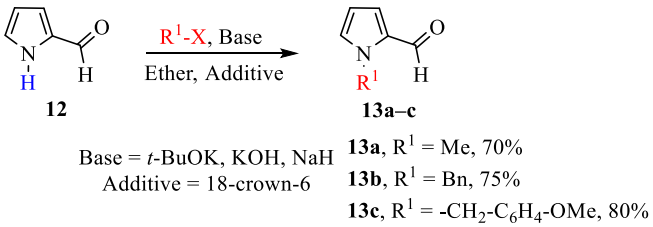

Scheme 4. Synthetic route of N-substituted pyrrole-2-carbaldehydes **13a-c**

4.1.2 Synthesis of azaindole derivatives (14a-d)

Azaindole cores were synthesized via a one-pot condensation-hetero-annulation of iminoester. Under solvent-free conditions, N-substituted pyrrole-2-carbaldehyde **13** reacts with the glycine methyl ester HCl salt in the presence of DIPEA base at 150 °C temperature in a sealed tube for 6-8 h to afford 1**4a-d** (Scheme 5).

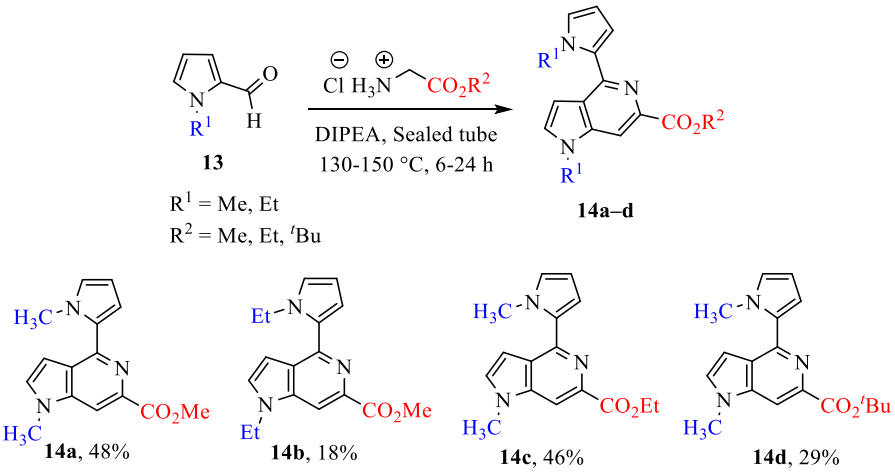

Scheme 5. Synthetic route of 5-azaindole derivatives **14a-d**

4.1.3 Synthesis of 1-methyl-4-(1-methyl-1H-pyrrol-2-yl)-6-((prop-2-yn-1-yloxy)methyl)-1H- pyrrolo[3,2-c]pyridine

The azaindole derivative **14a** was reduced by $LiAlH_4$ in a polar aprotic solvent (THF) to obtain the corresponding primary alcohol **15** respectively. Alcohol **15** was propargylated using a strong base, NaH by generating alkoxide ion, and the subsequent nucleophilic substitution reaction with propargyl bromide to give the terminal alkyne **16** (Scheme 6).

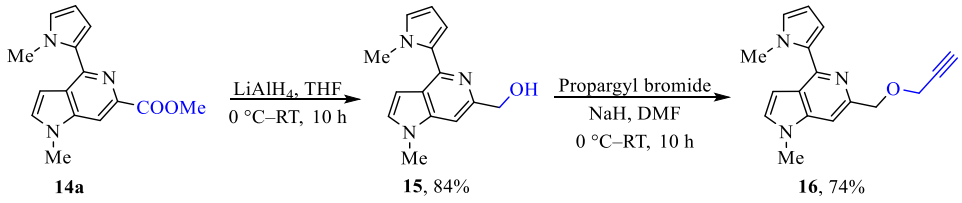

Scheme 6. Synthetic route of terminal alkyne derivative **16**

4.1.4 Synthesis of azido derivatives of isatin

Isatin **17** was treated with 1,2-dibromoethane in the presence of K_2CO_3 in DMF to obtain substituted N-(2-bromoethyl)indoline-2,3-diones **18a-d**. Azide group replaces bromide atom in **18a-d** by the reaction with

sodium azide in DMF for 12-16 h at room temperature to afford **19a-d** (Scheme 7).

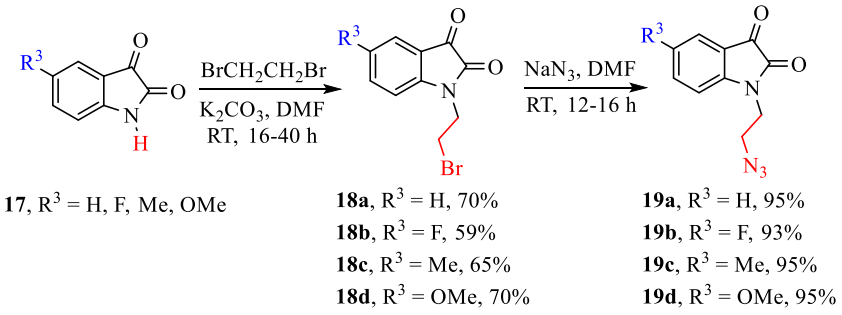

Scheme 7. Synthetic route for azido isatin derivatives **19a-d**

4.1.5 Synthesis of pyrrolo[3,2-c]pyridine-isatin hybrids

The final step for this multistep synthesis involves the coupling of terminal alkynes **16** and azide **19a** by standard click reaction, using monohydrated copper acetate as a catalyst for 1,3-dipolar cycloaddition and sodium ascorbate in DMF solvent at room temperature to afford the final molecule pyrrolopyridine-isatin hybrids **20**, **21** (Scheme 8).

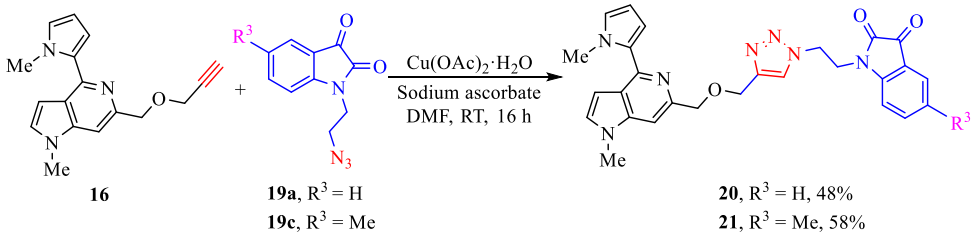

Scheme 8. Synthetic route for triazole-tethered pyrrolopyridine-isatin hybrids **20**, **21**

4.2 Possible mechanism of the formation of 5-azaindole core

Initially, trans iminoester formed from the N-substituted pyrrole-2-aldehyde **13** and glycine methyl ester. A carbon nucleophile generates in presence of Hunig's base (DIPEA) by abstracting an active methylene proton from the trans iminoester. It undergoes a nucleophilic addition reaction with another molecule of N-substituted pyrrole-2-carbaldehyde

13 and intermediate imino alcohol is obtained. The obtained iminoalcohol eliminates water molecule to give an iminoenamine intermediate. It may go through ring closure following path a or path b. In the path a, imine nitrogen of the intermediate iminoenamine is protonated by the conjugate acid (+BH) generating an iminium intermediate. It further undergoes an electrophilic substitution reaction at position-3 of the pyrrole moiety and a second carbon–carbon bond is formed. This intermediate further aromatizes through deprotonation to obtain 4,6-disubstituted 4,5-dihydroazaindole. In path b, it undergoes a thermal 6-π electrocyclic reaction to obtain 4,6-disubstituted 4,8-dihydroazaindole. In situ dehydrogenation of 4,6-disubstituted 4,5-dihydroazaindole or 4,6-disubstituted 4,8-dihydroazaindole through aerial oxidation produces desired products 4,6-disubstituted-5-azaindoles.

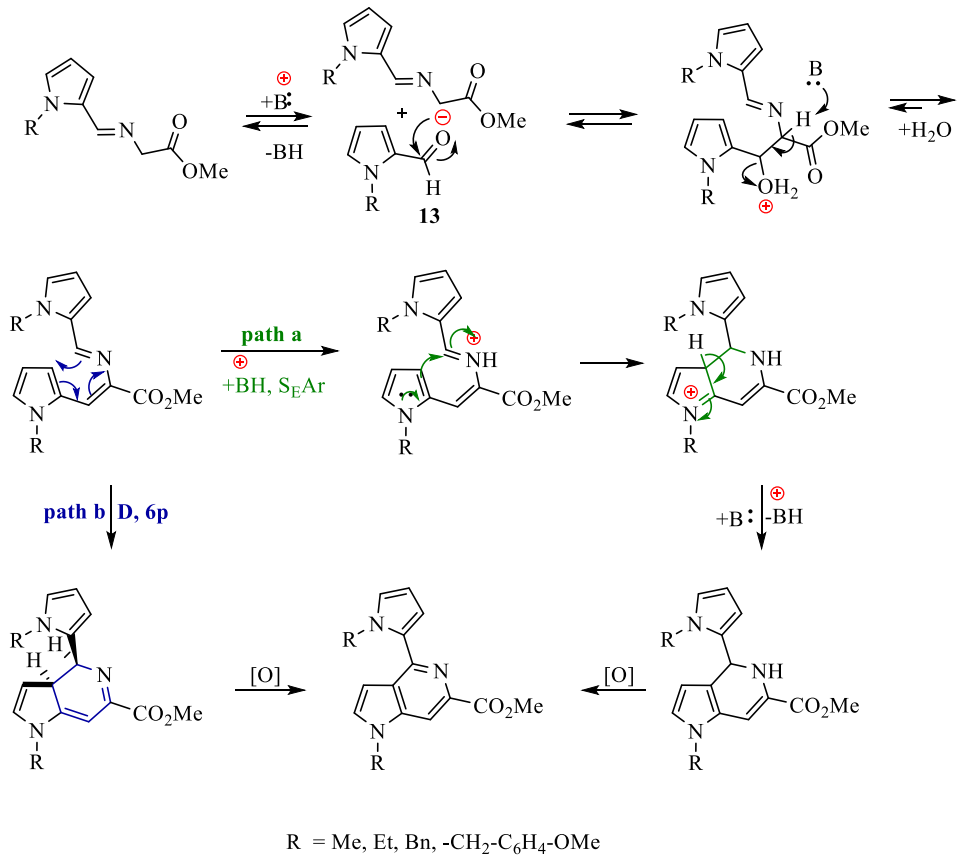

Scheme 9. Possible mechanism for the formation of 5-azaindole core

Chapter 5

CONCLUSIONS

In conclusion, we have successfully synthesized two hybrids 1-(2-(4-(((1-Methyl-4-(1-methyl-1H-pyrrol-2-yl)-1H-pyrrolo[3,2-c]pyridin-6-yl)methoxy)methyl)-1H-1,2,3-triazol-1-yl)ethyl)indoline-2,3-dione (**20**) and 5-methyl-1-(2-(4-(((1-methyl-4-(1-methyl-1H-pyrrol-2-yl)-1H-pyrrolo[3,2-c]pyridin-6-yl)methoxy)methyl)-1H-1,2,3-triazol-1-yl)ethyl)indoline-2,3-dione (**21**) through standard click chemistry reaction and several intermediates. The compounds are thoroughly characterized using various spectroscopic techniques such as ^{1}H, ^{13}C NMR, and HR-MS.

These triazole-tethered pyrrolopyridine-isatin hybrids will serve as competitive inhibitors of polyketide synthetase 13 (Pks13), inhibiting mycolic acid synthesis. The activity of the hybrid compounds against MDR and XDR tuberculosis will be investigated further. This may lead to the discovery of new potent drugs against drug-resistant tuberculosis. Designing more potent anti-TB molecules of this series is currently underway in our research group.

APPENDIX A

HR-MS, ^{1}H NMR, and ^{13}C NMR spectra of compounds are enlisted below.

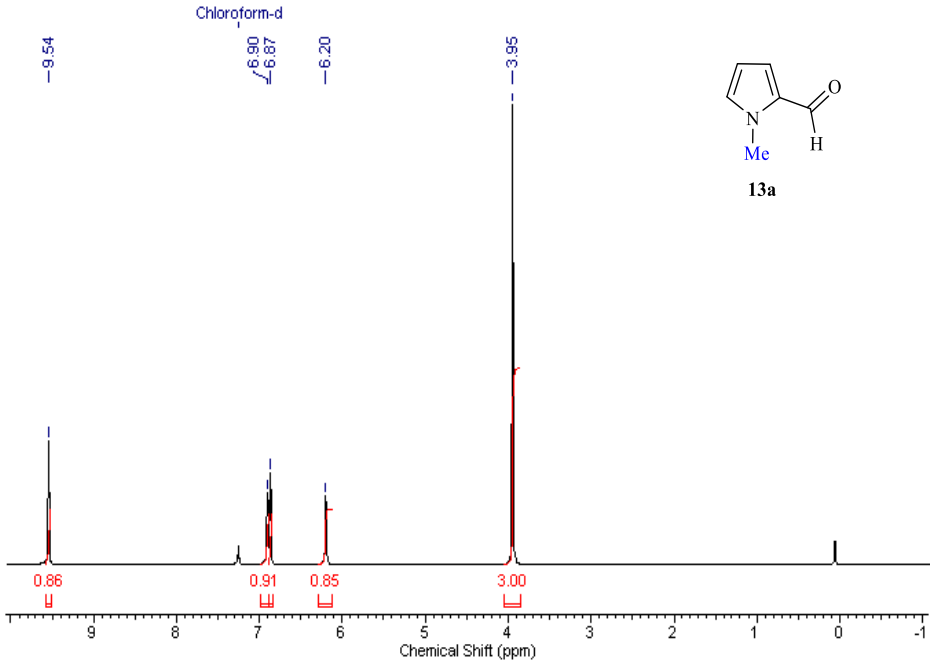

Figure 5. ^{1}H NMR spectrum of **13a** in $CDCl_3$

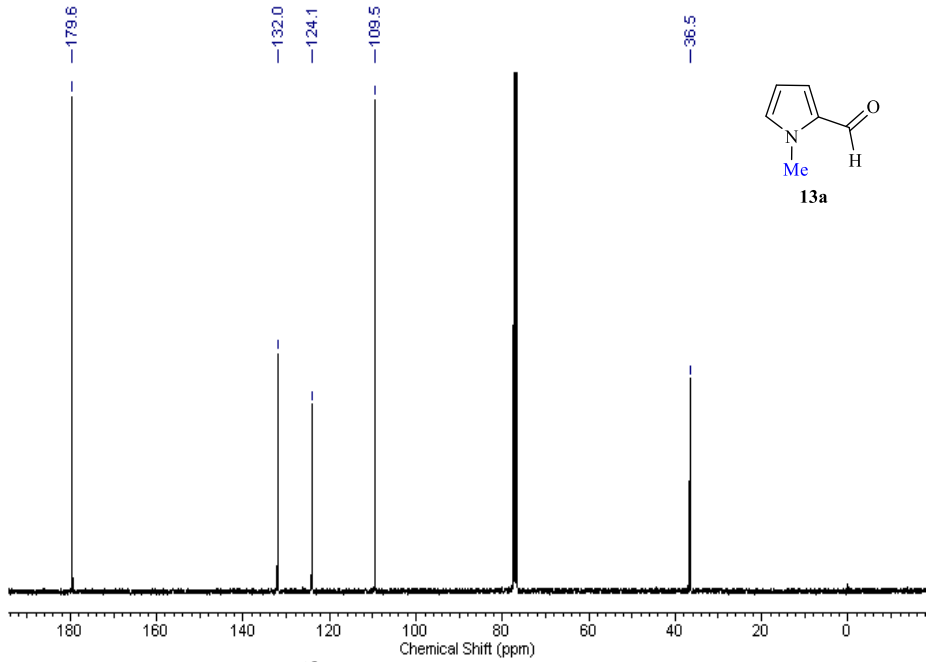

Figure 6. ^{13}C NMR spectrum of **13a** in $CDCl_3$

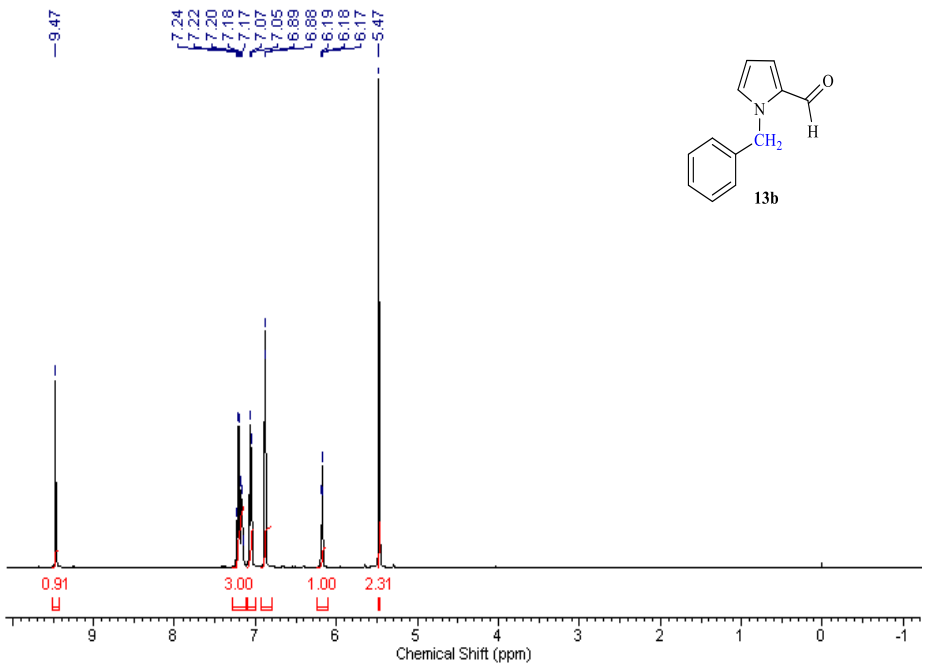

Figure 7. ^{1}H NMR spectrum of **13b** in $CDCl_3$

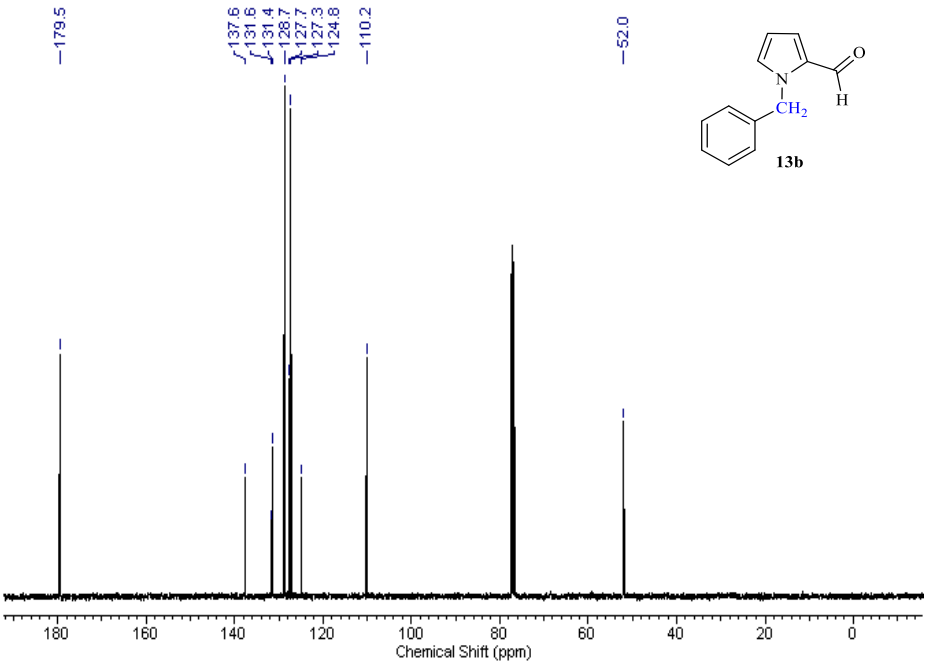

Figure 8. ^{13}C NMR spectrum of **13b** in $CDCl_3$

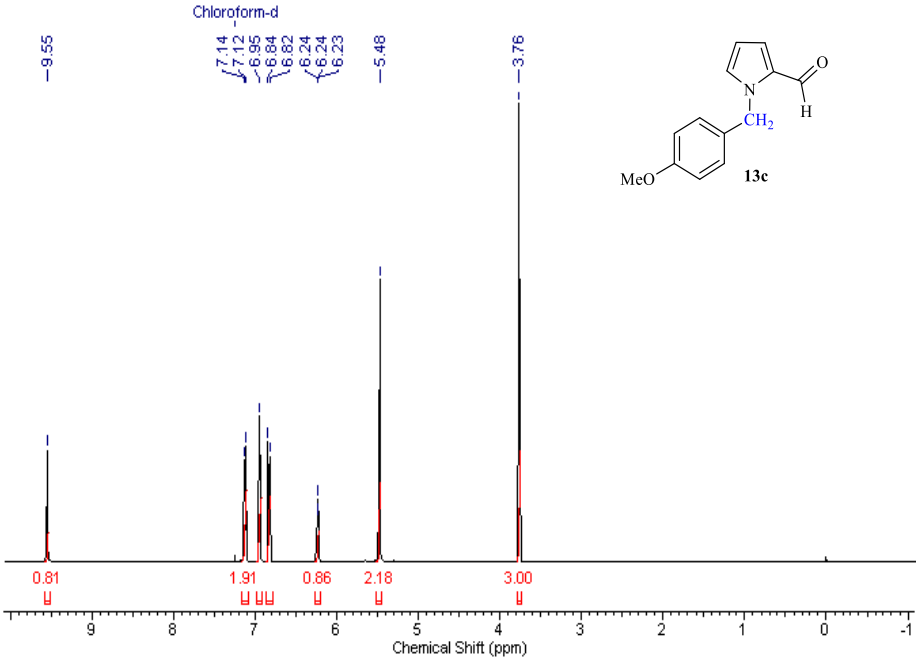

Figure 9. ^{1}H NMR spectrum of **13c** in $CDCl_3$

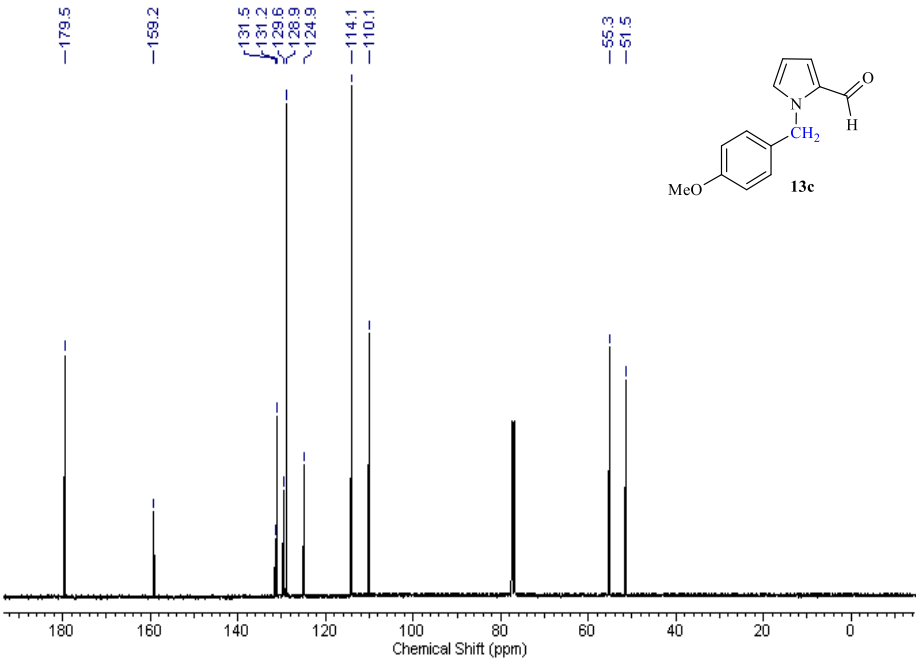

Figure 10. ^{13}C NMR spectrum of **13c** in $CDCl_3$

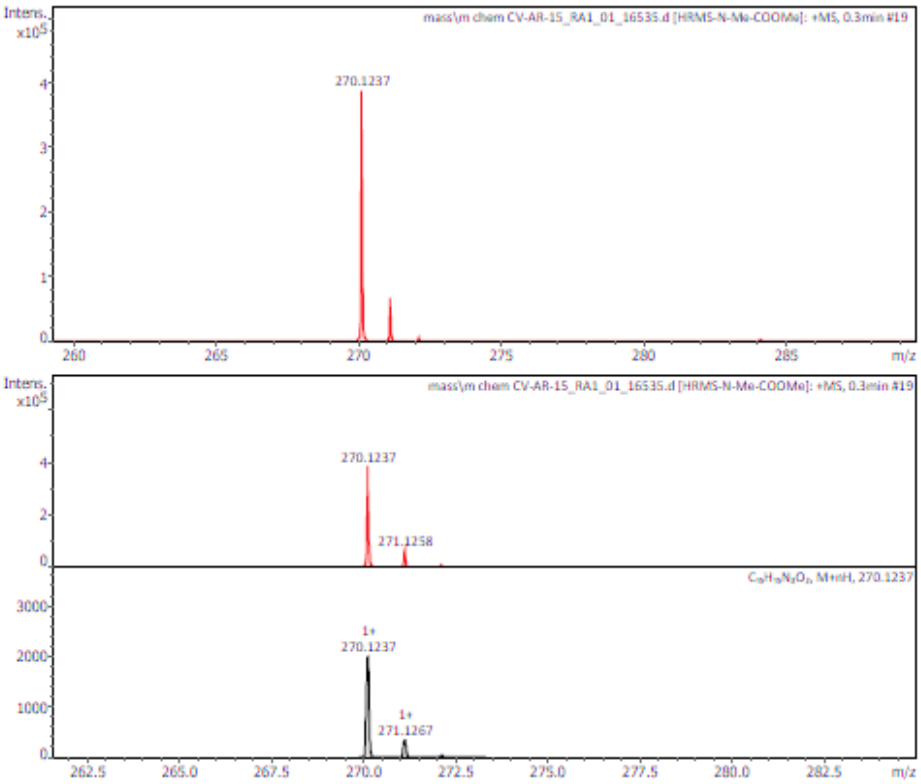

Figure 11. HR-MS of **14a** in MeOH

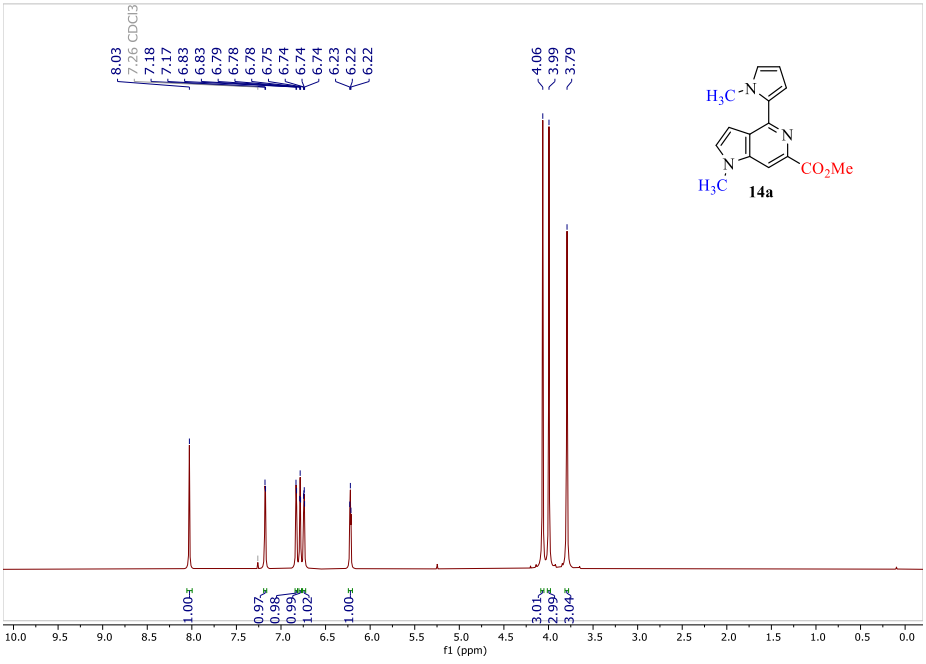

Figure 12. ^{1}H NMR spectrum of **14a** in $CDCl_3$

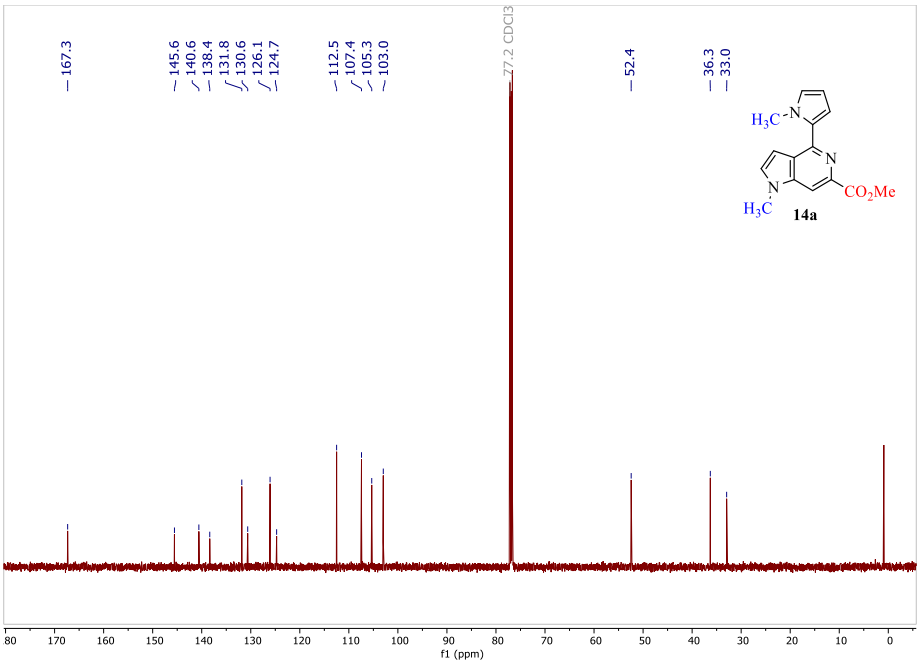

Figure 13. ^{13}C NMR spectrum of **14a** in $CDCl_3$

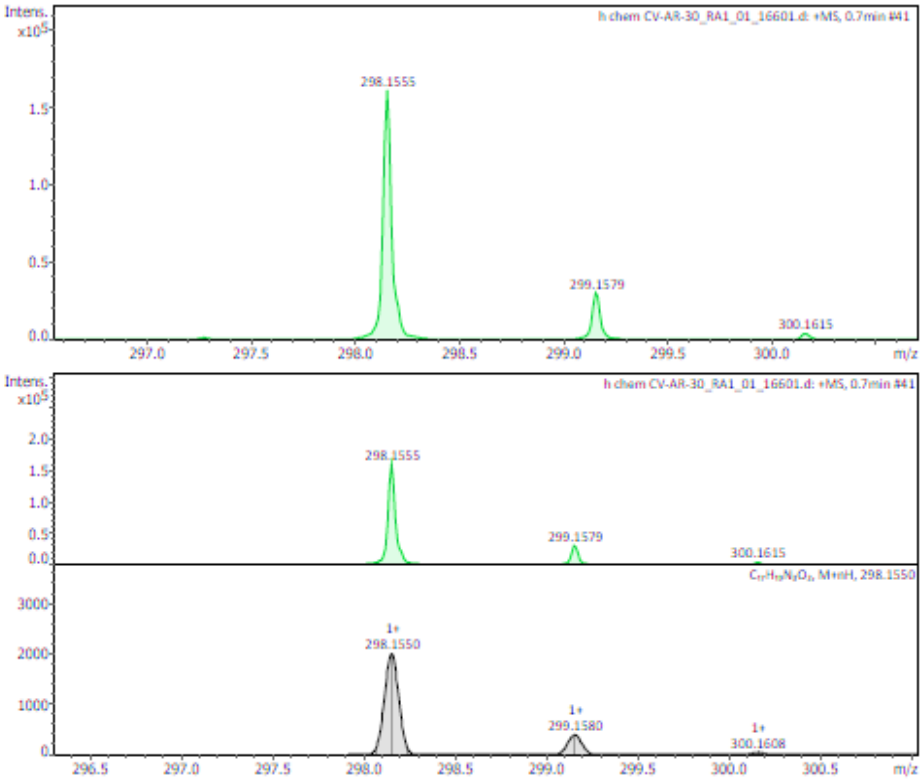

Figure 14. HR-MS of **14b** in MeOH

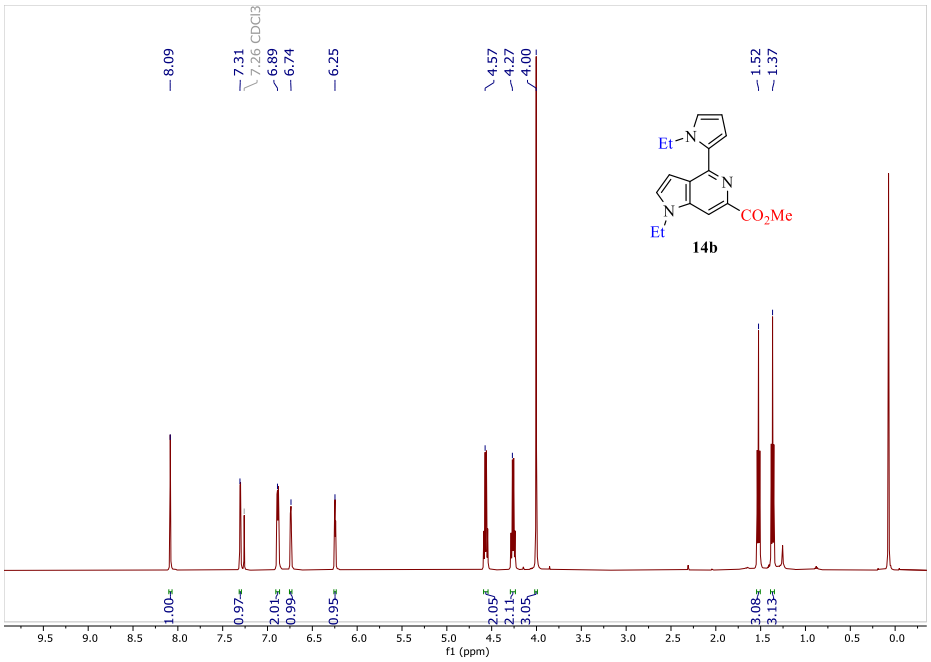

Figure 15. ^{1}H NMR spectrum of **14b** in $CDCl_3$

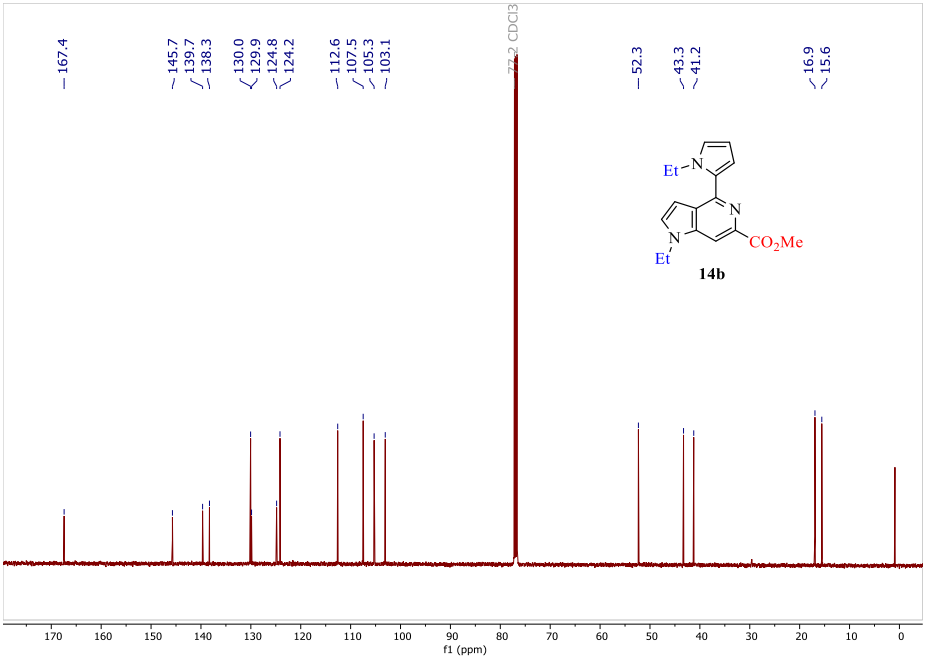

Figure 16. ^{13}C NMR spectrum of **14b** in $CDCl_3$

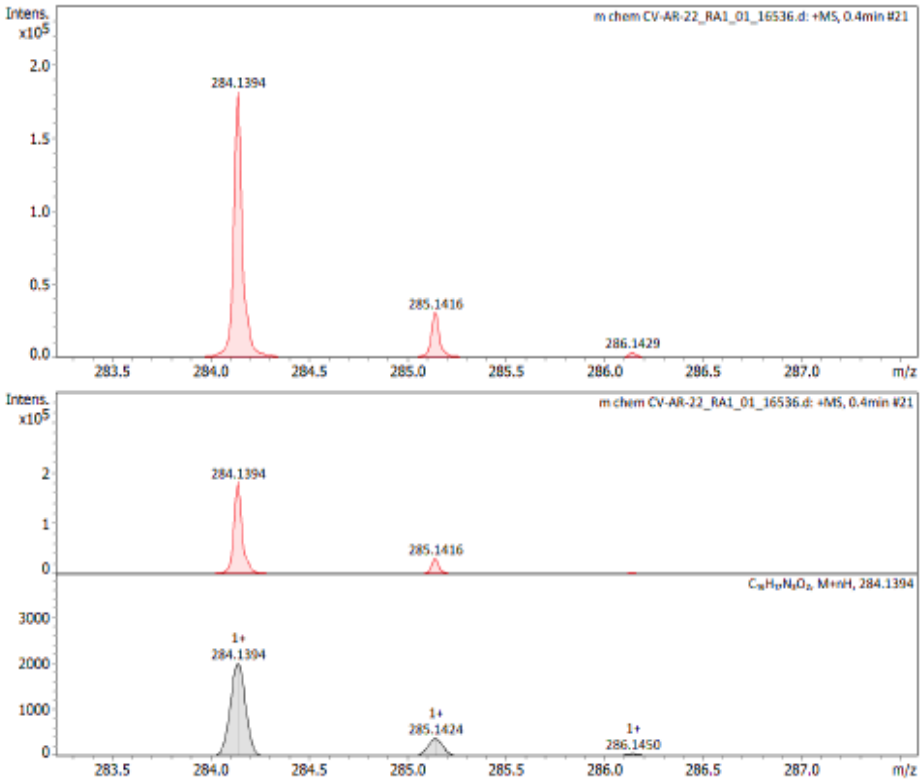

Figure 17. HR-MS of **14c** in MeOH

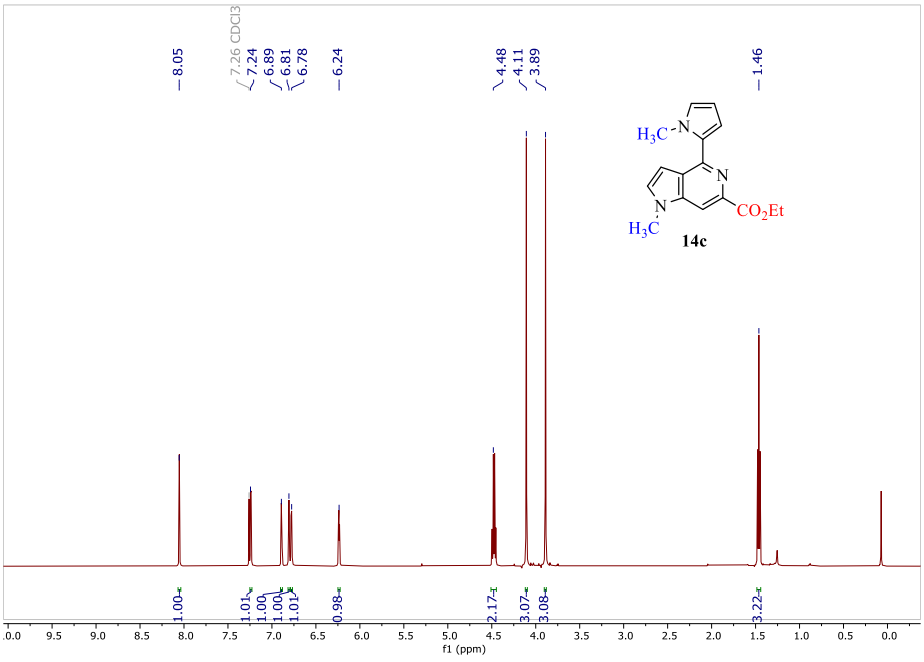

Figure 18. ^{1}H NMR spectrum of **14c** in $CDCl_3$

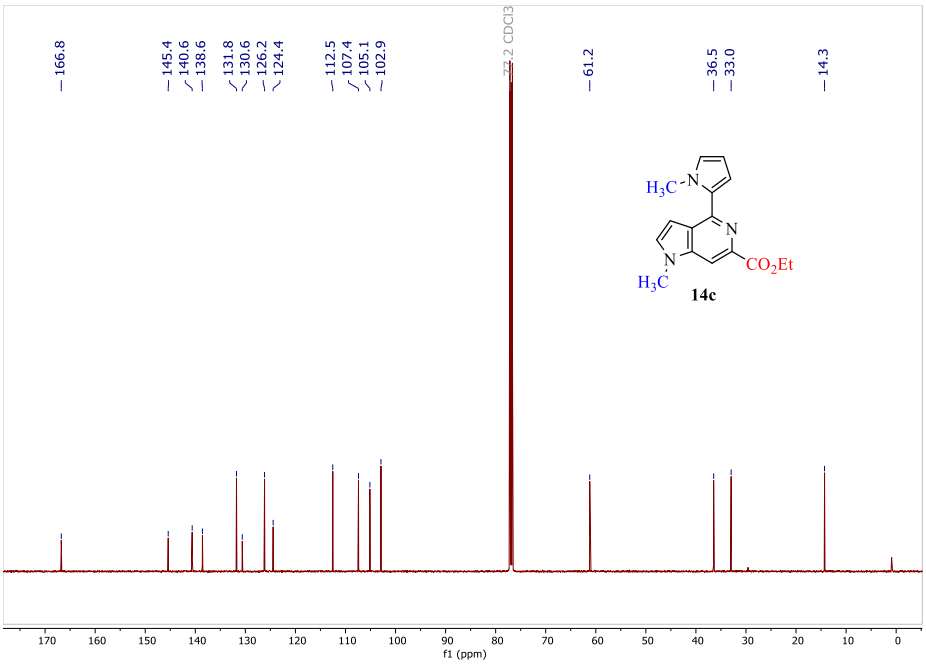

Figure 19. ^{13}C NMR spectrum of **14c** in $CDCl_3$

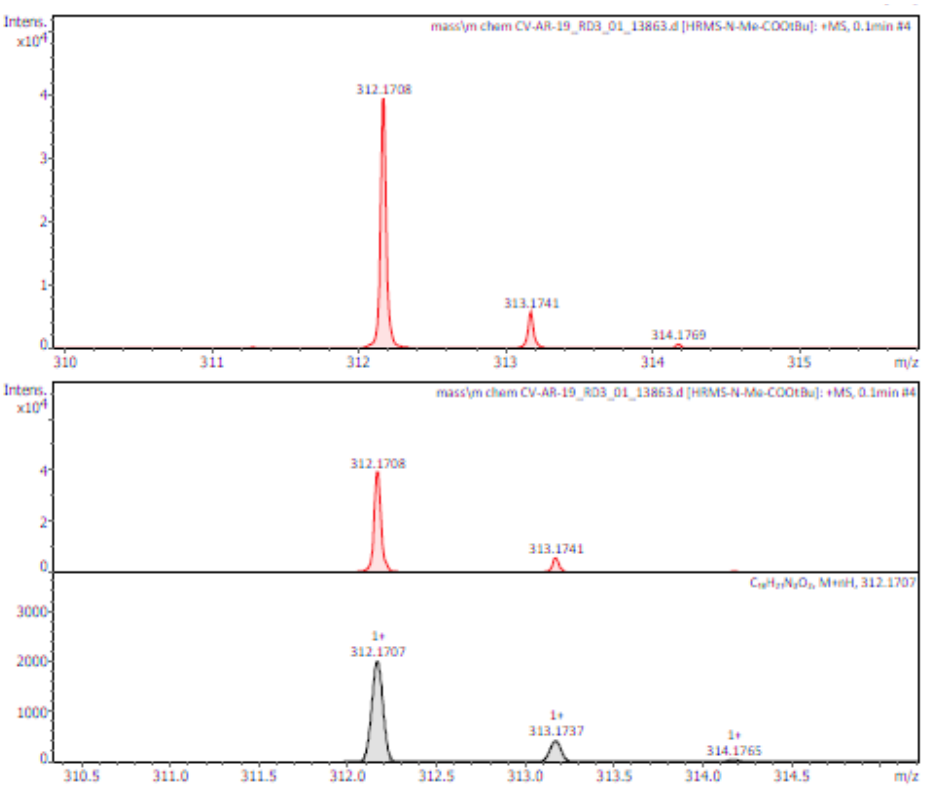

Figure 20. HR-MS of **14d** in MeOH

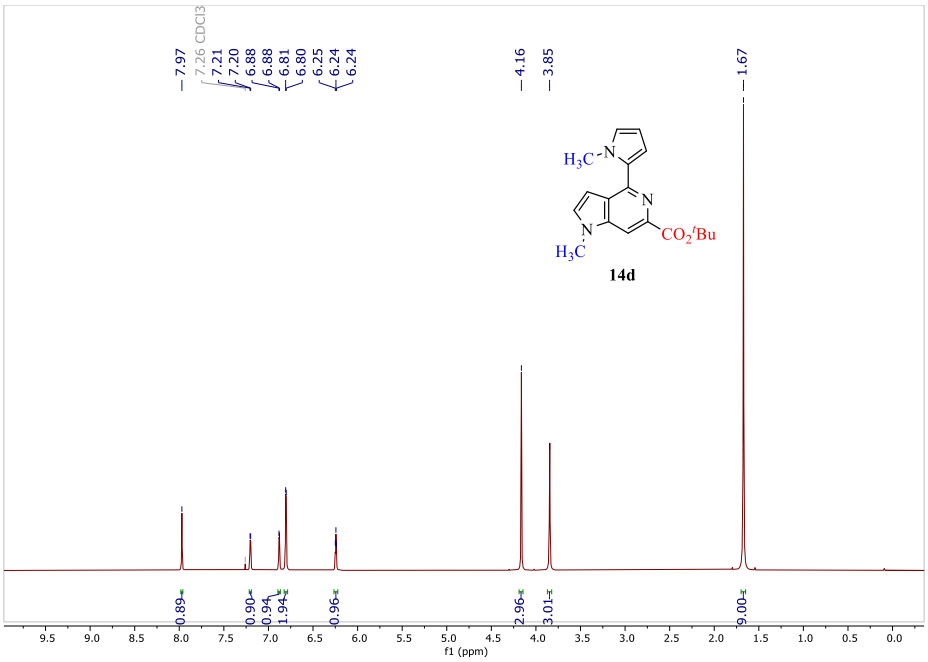

Figure 21. ^{1}H NMR spectrum of **14d** in $CDCl_3$

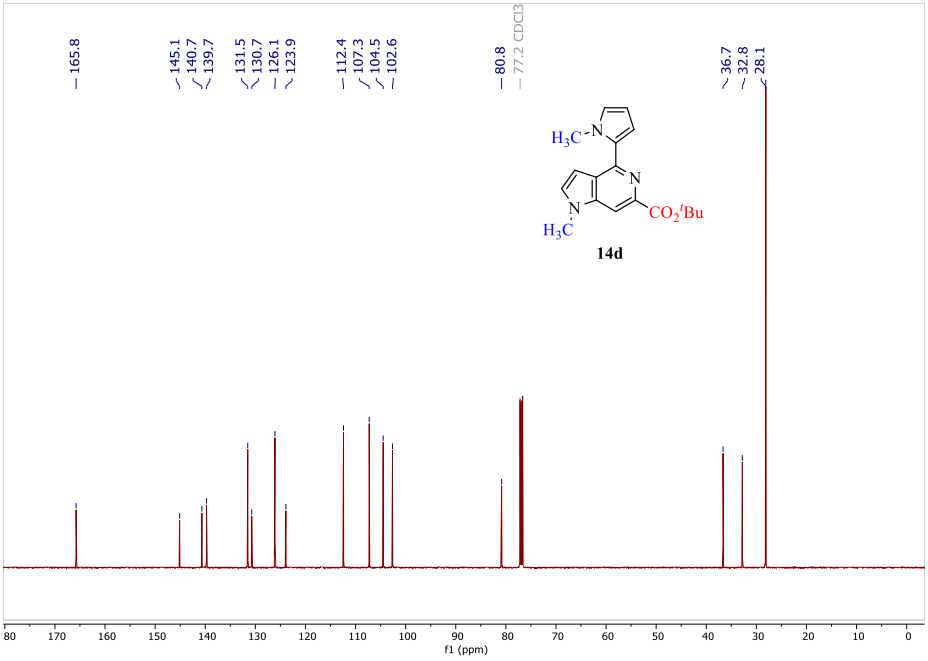

Figure 22. ^{13}C NMR spectrum of **14d** in $CDCl_3$

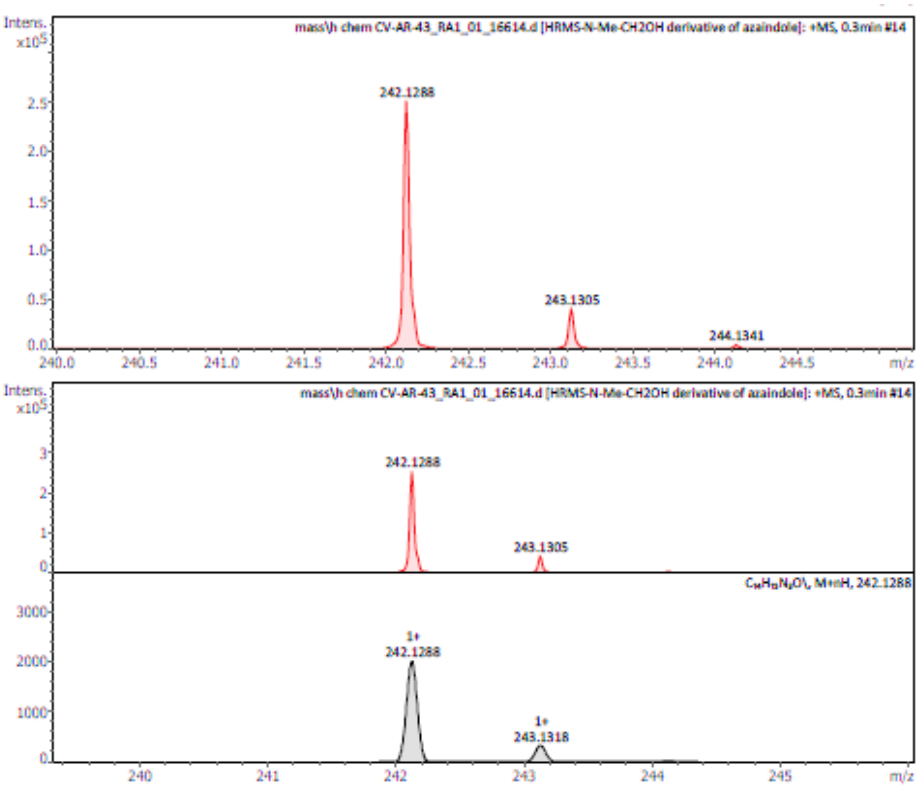

Figure 23. HR-MS of **15** in MeOH

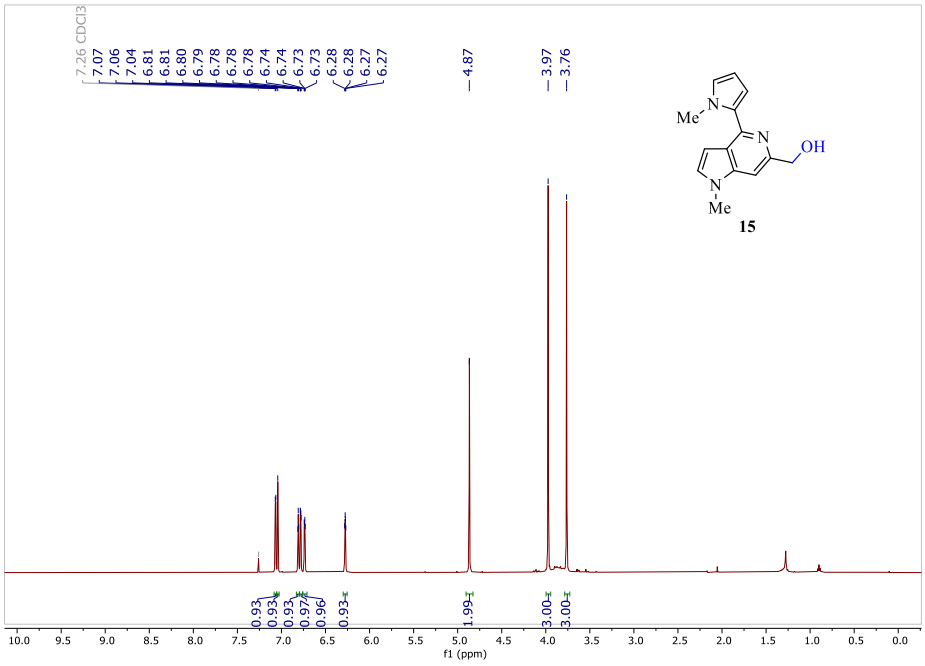

Figure 24. ^{1}H NMR spectrum of **15** in $CDCl_3$

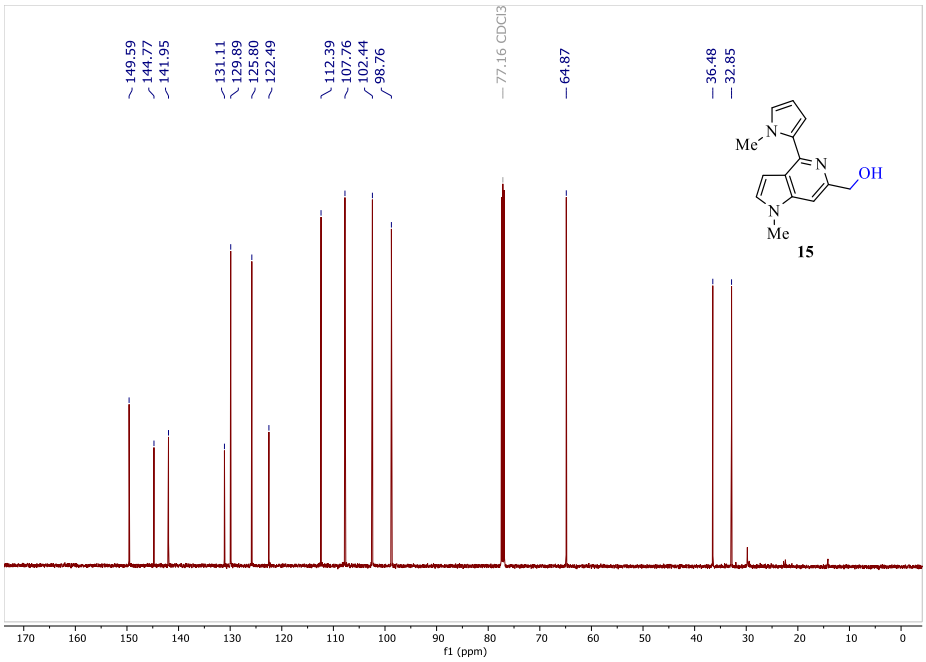

Figure 25. ^{13}C NMR spectrum of **15** in $CDCl_3$

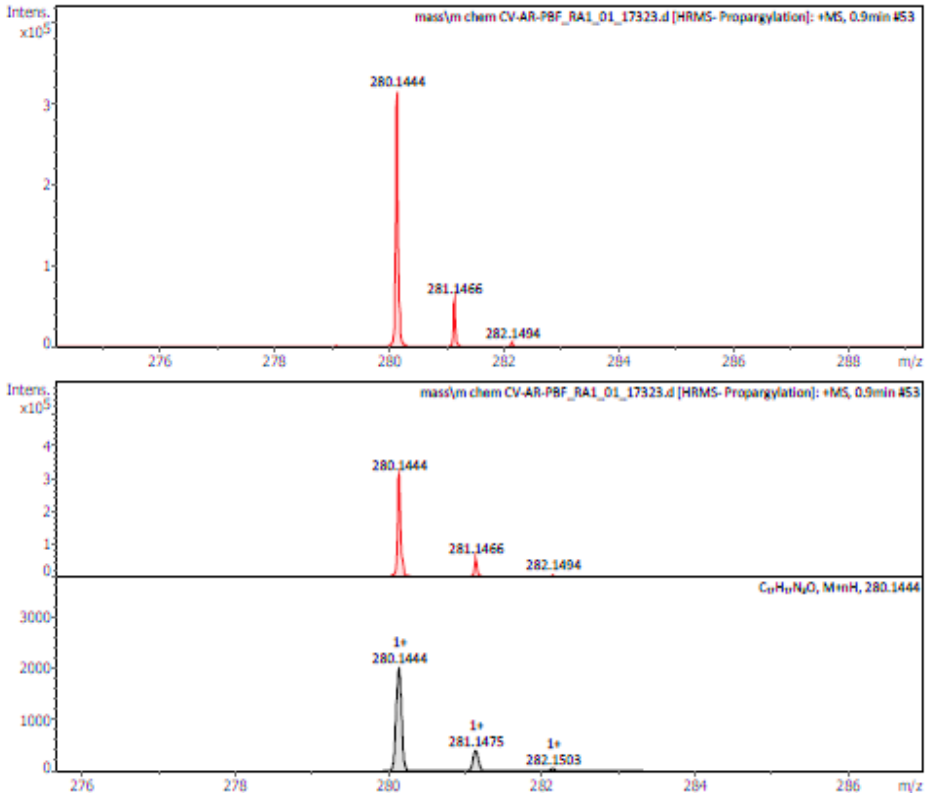

Figure 26. HR-MS of **16** in MeOH

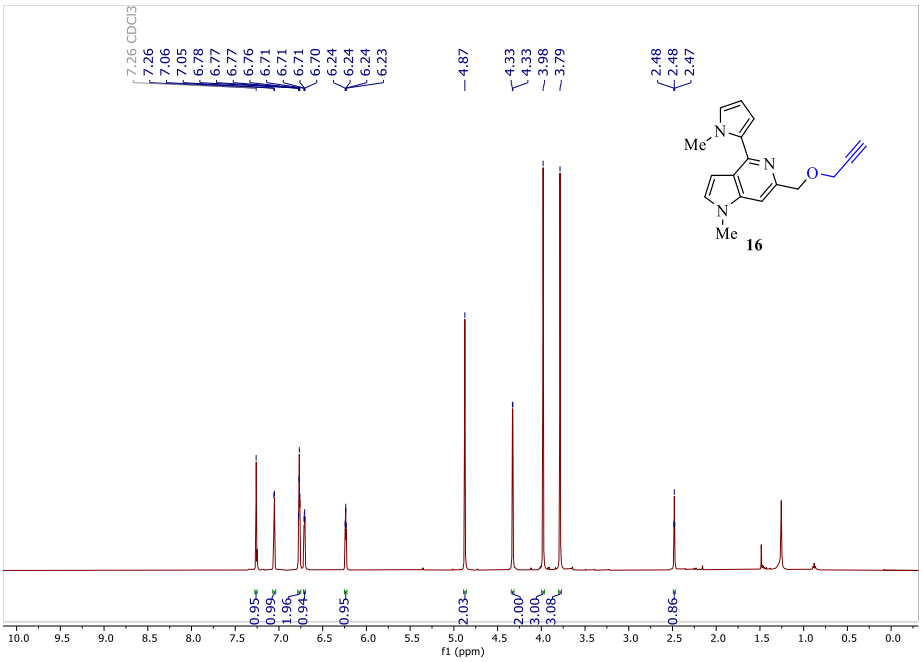

Figure 27. ^{1}H NMR spectrum of **16** in $CDCl_3$

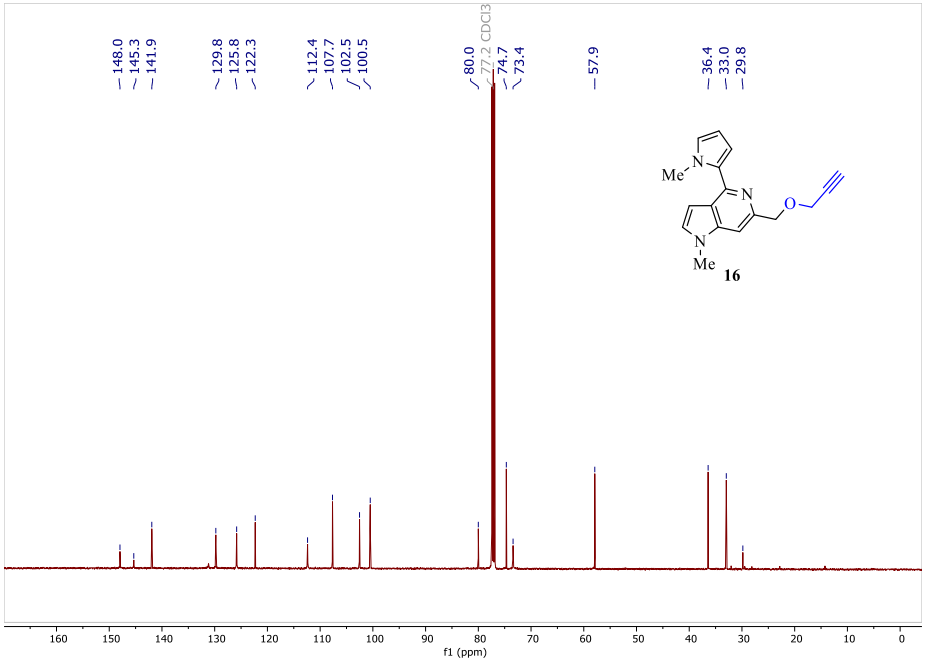

Figure 28. ^{13}C NMR spectrum of **16** in $CDCl_3$

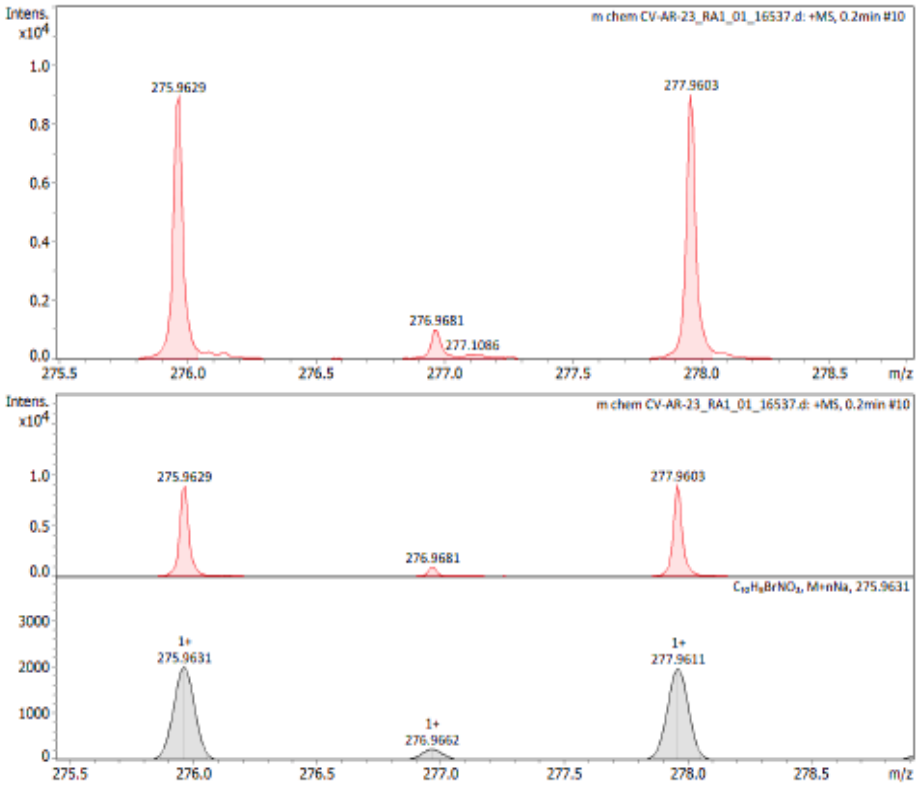

Figure 29. HR-MS of **18a** in MeOH

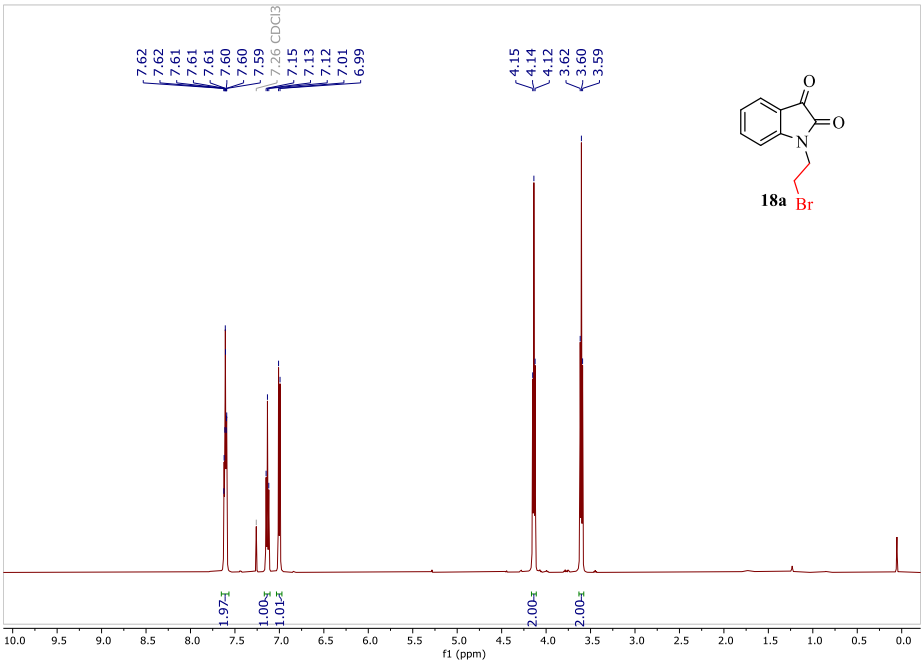

Figure 30. ^{1}H NMR spectrum of **18a** in $CDCl_3$

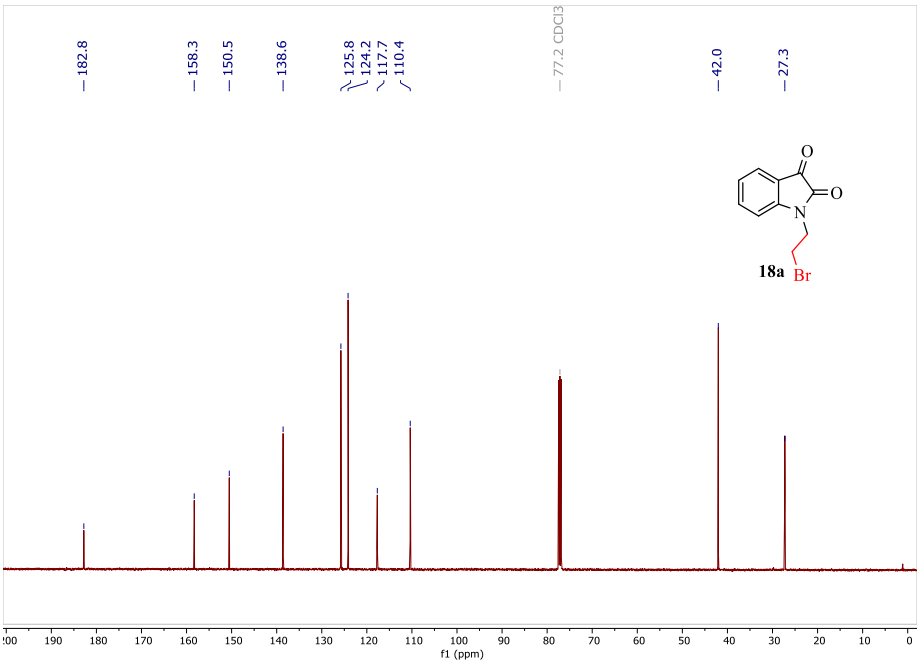

Figure 31. ^{13}C NMR spectrum of **18a** in $CDCl_3$

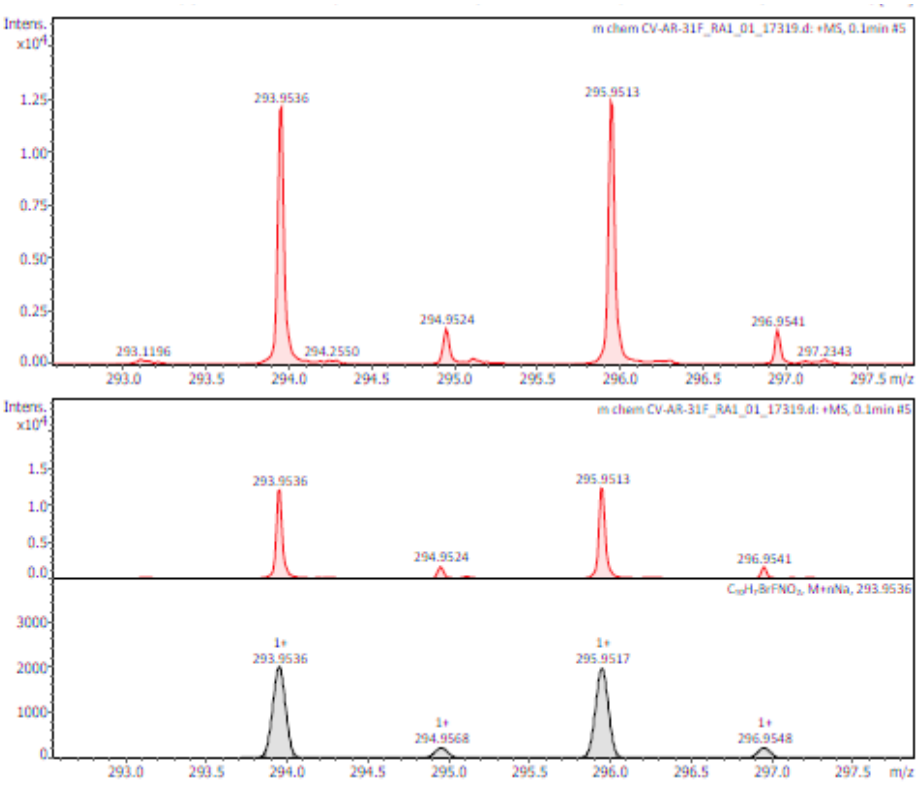

Figure 32. HR-MS of **18b** in MeOH

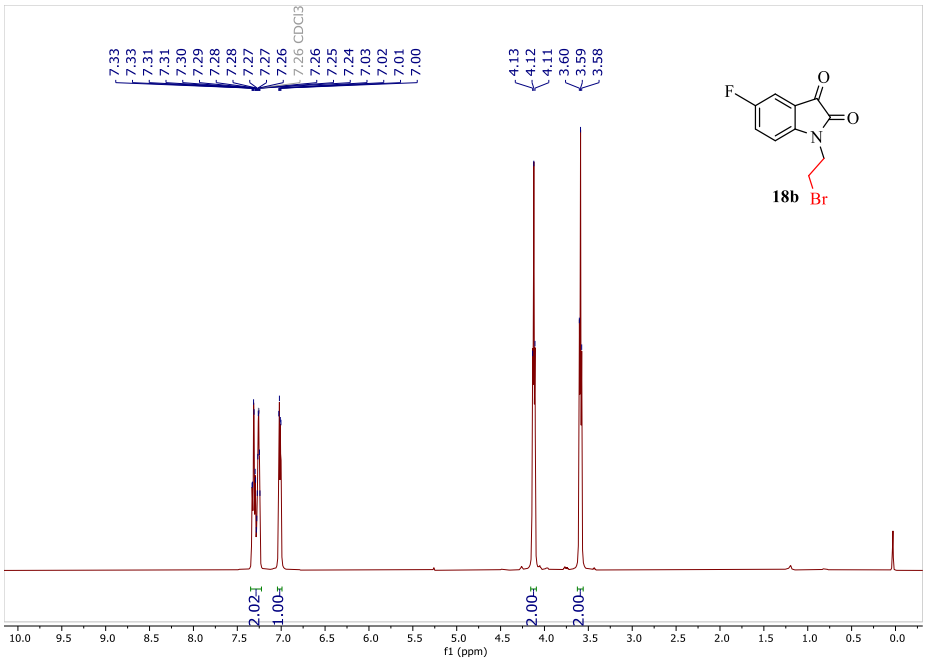

Figure 33. ^{1}H NMR spectrum of **18b** in $CDCl_3$

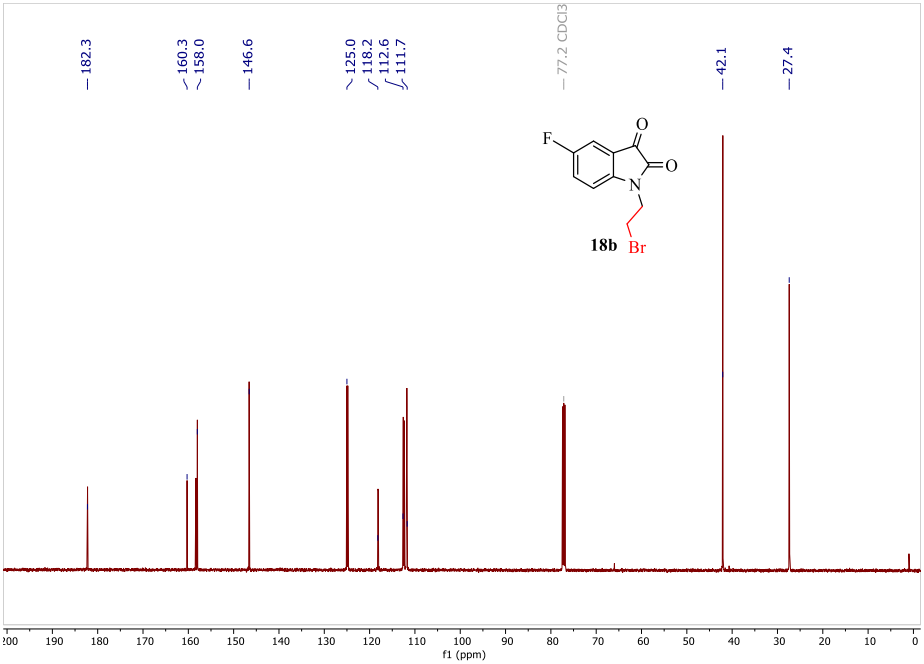

Figure 34. ^{13}C NMR spectrum of **18b** in $CDCl_3$

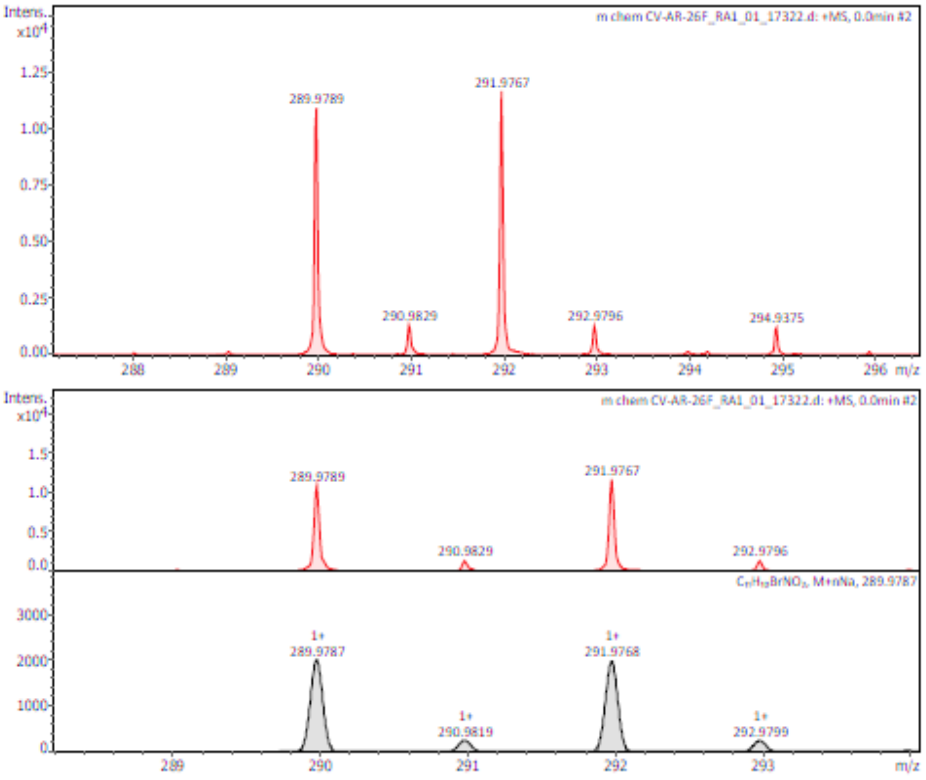

Figure 35. HR-MS of **18c** in MeOH

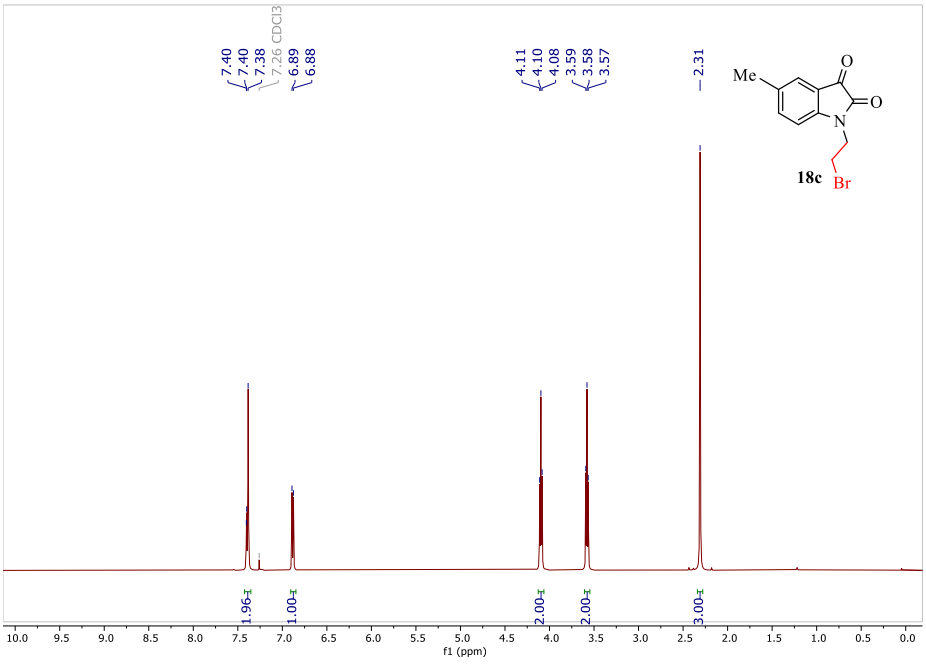

Figure 36. ^{1}H NMR spectrum of **18c** in $CDCl_3$

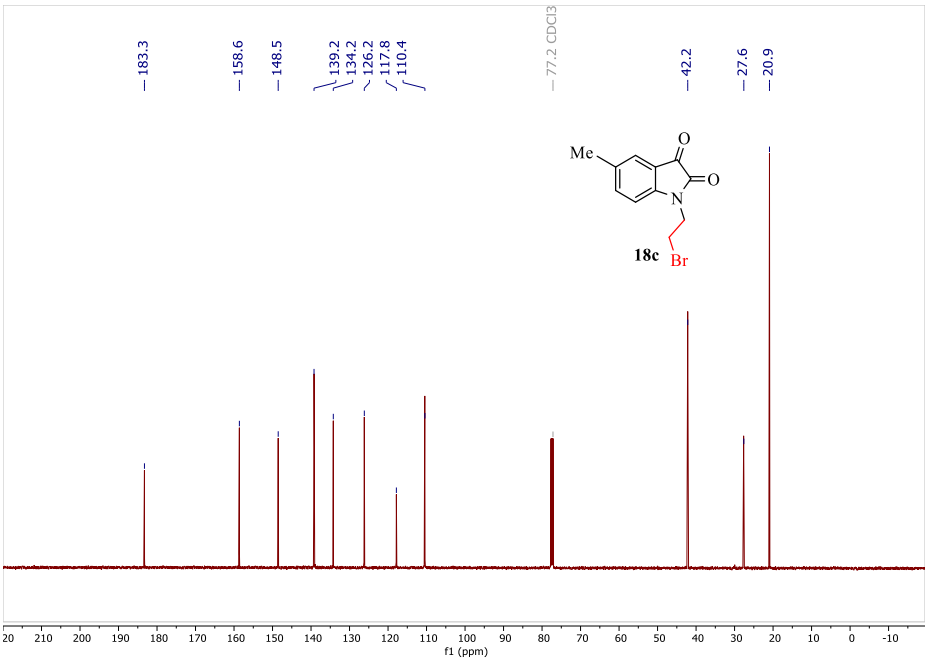

Figure 37. ^{13}C NMR spectrum of **18c** in $CDCl_3$

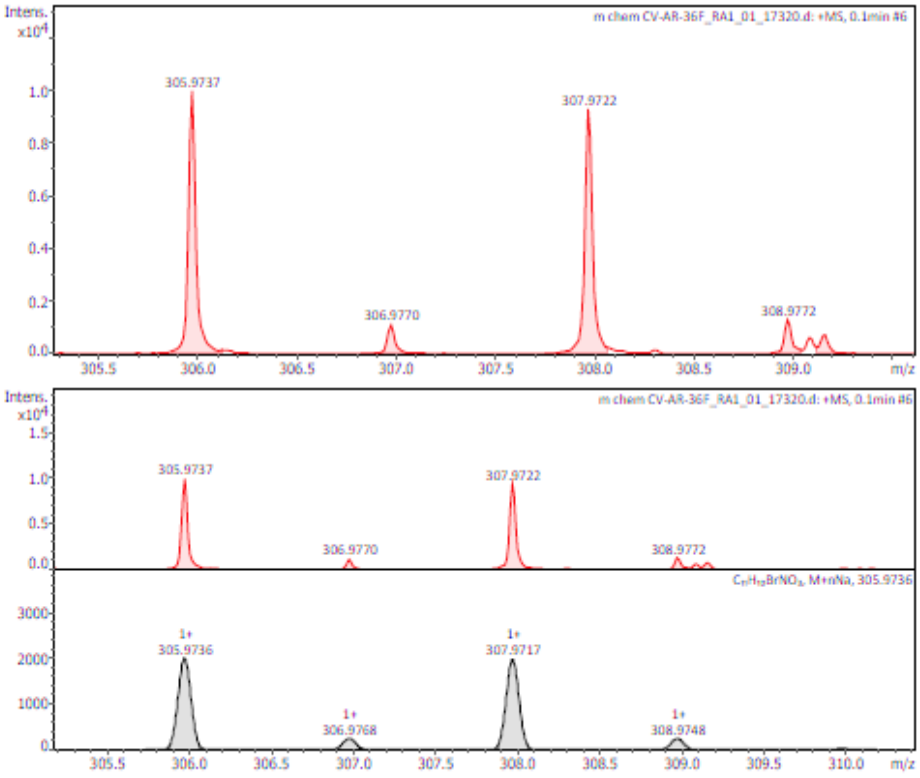

Figure 38. HR-MS of **18d** in MeOH

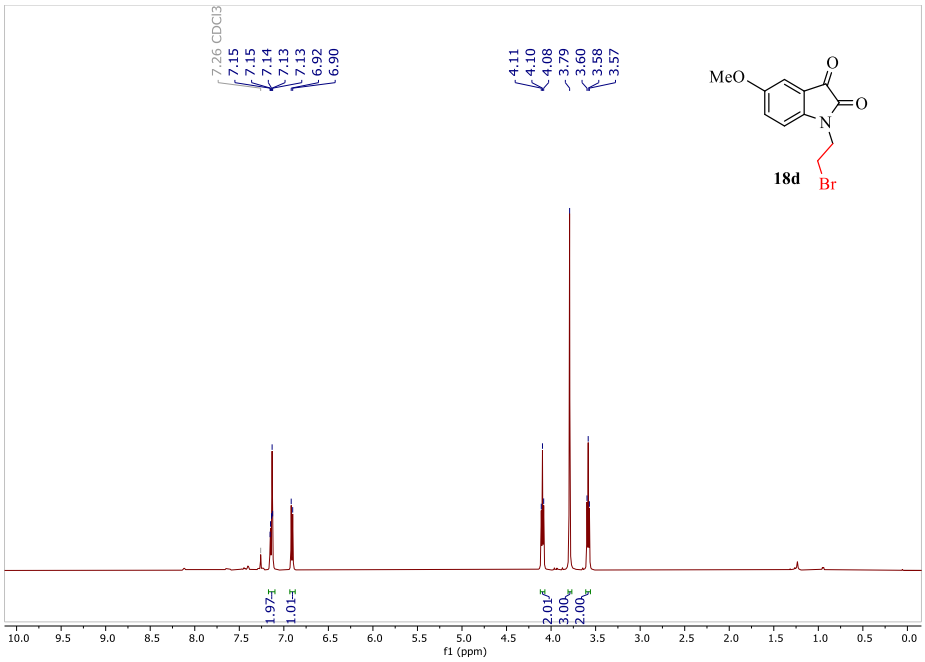

Figure 39. ^{1}H NMR spectrum of **18d** in $CDCl_3$

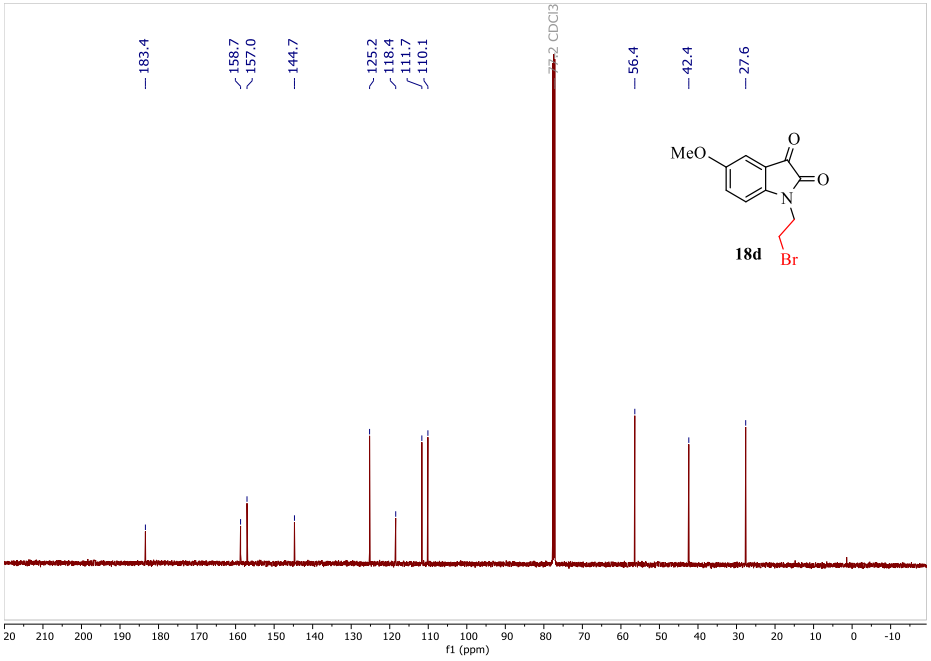

Figure 40. ^{13}C NMR spectrum of **18d** in $CDCl_3$

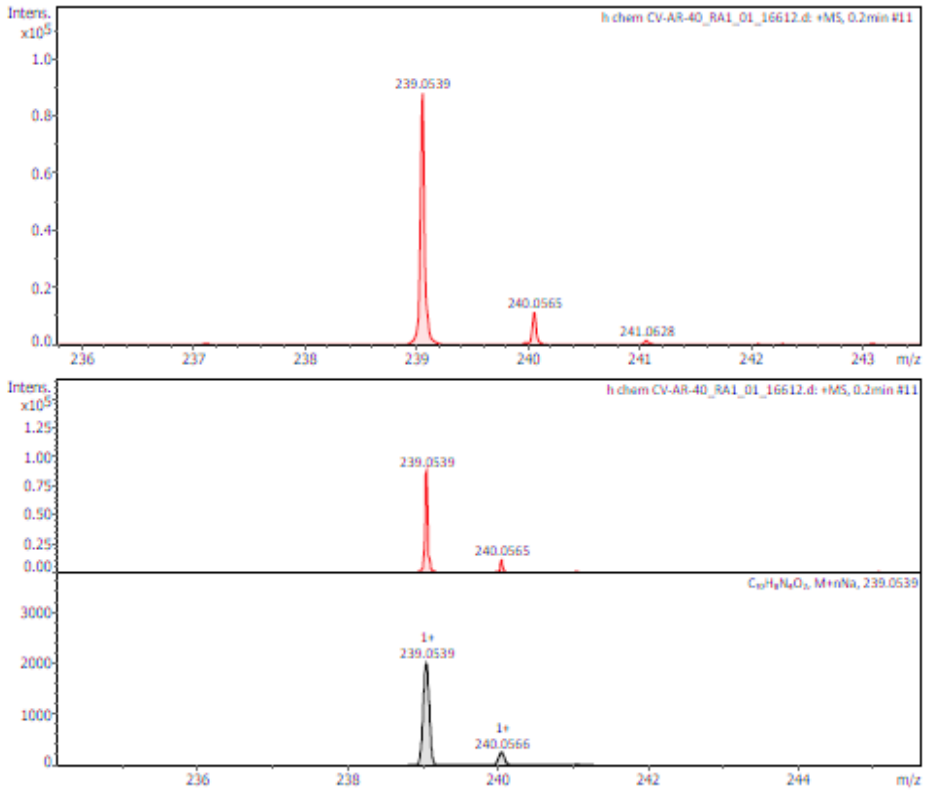

Figure 41. HR-MS of **19a** in MeOH

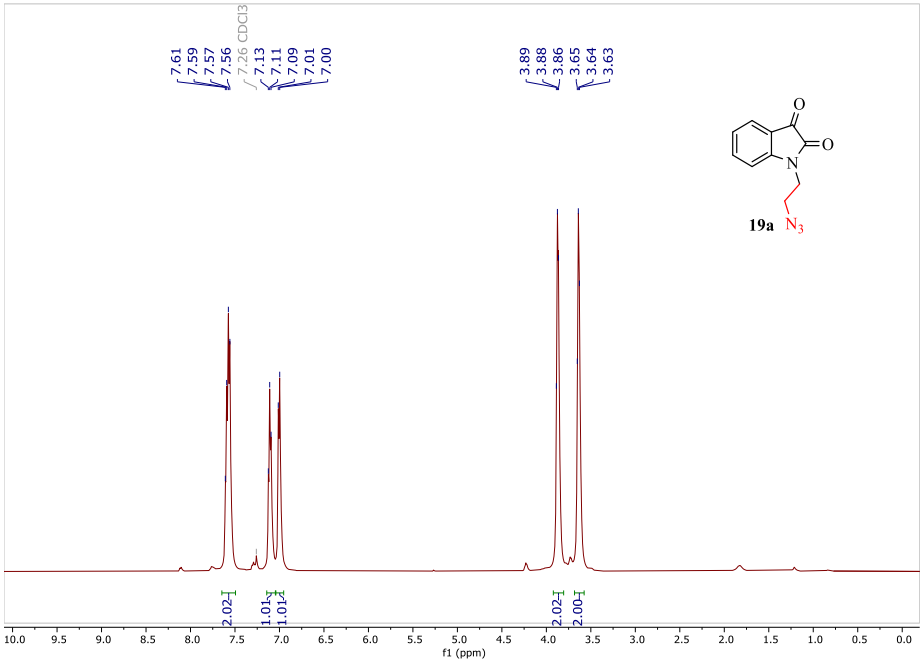

Figure 42. ^{1}H NMR spectrum of **19a** in $CDCl_3$

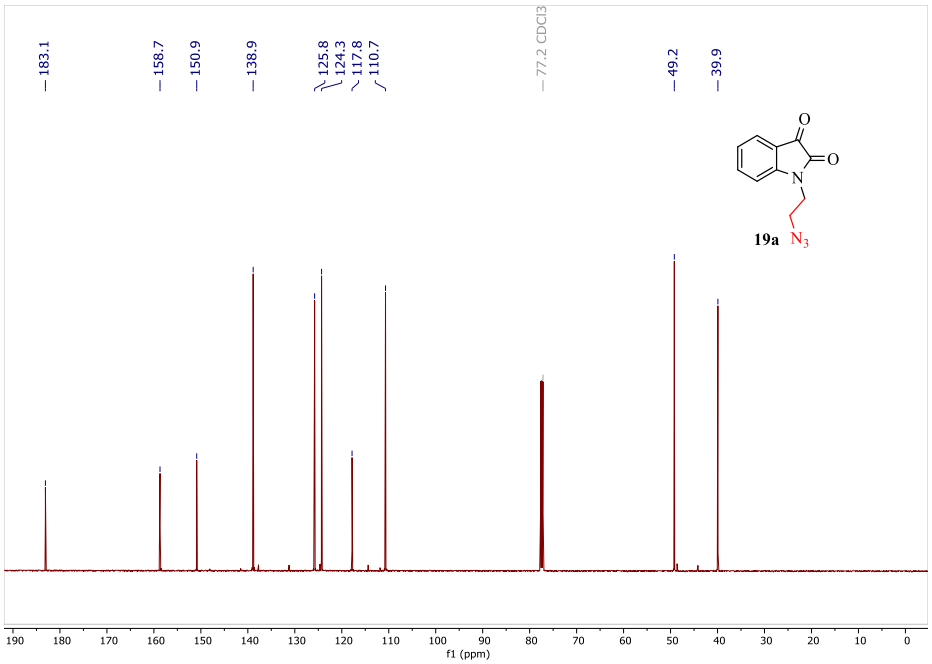

Figure 43. ^{13}C NMR spectrum of **19a** in $CDCl_3$

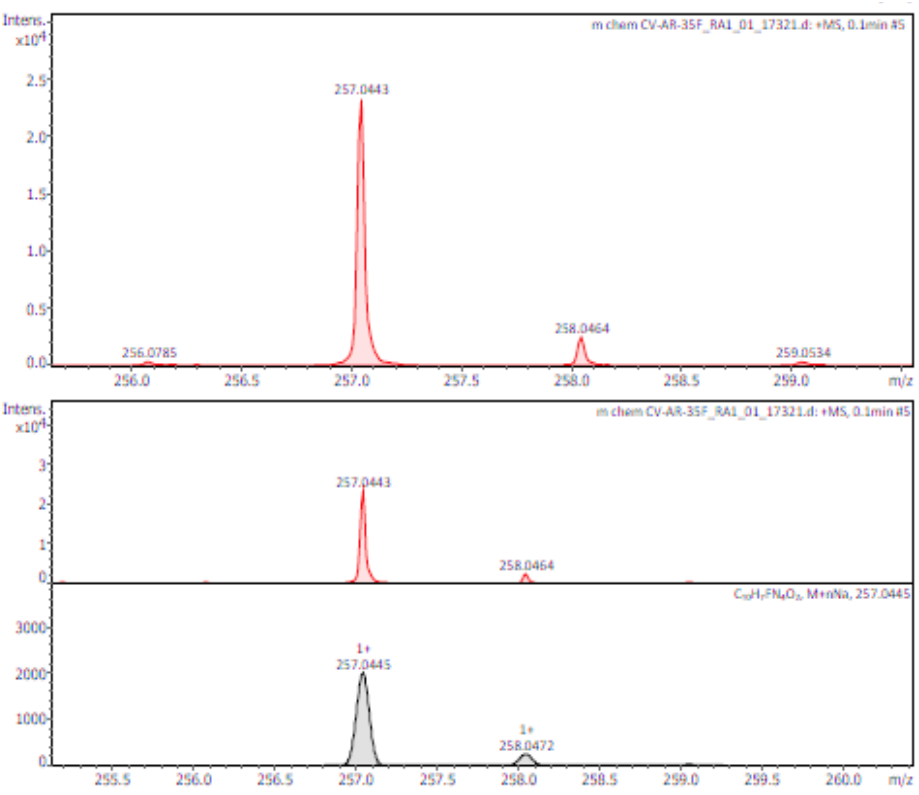

Figure 44. HR-MS of **19b** in MeOH

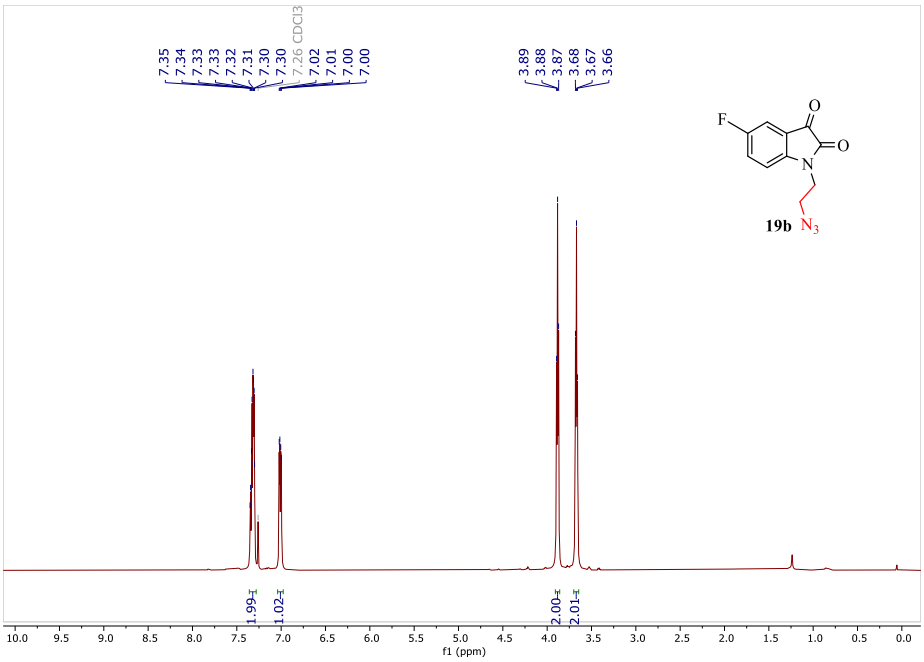

Figure 45. ^{1}H NMR spectrum of **19b** in $CDCl_3$

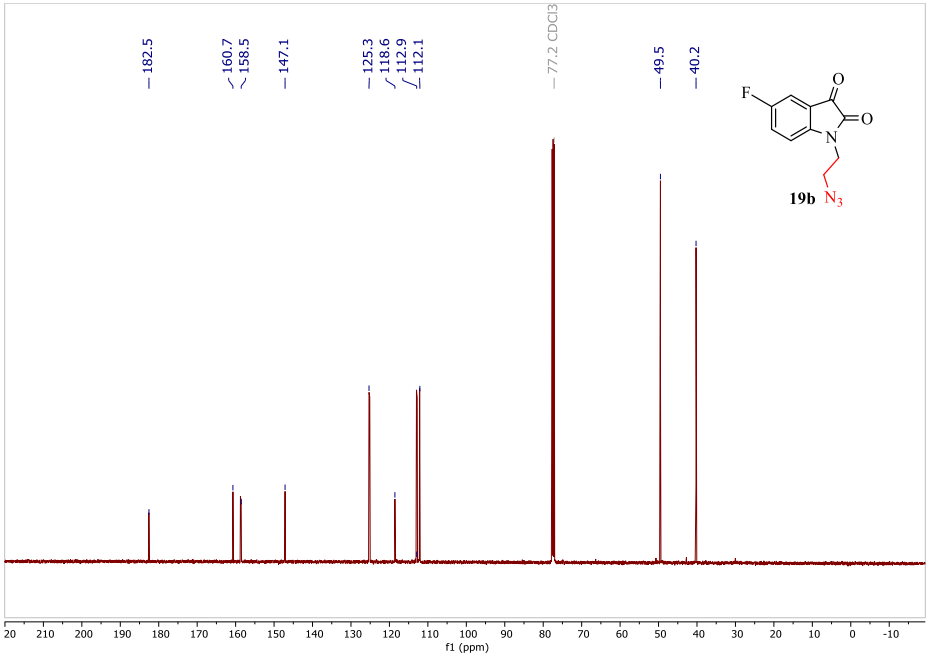

Figure 46. ^{13}C NMR spectrum of **19b** in $CDCl_3$

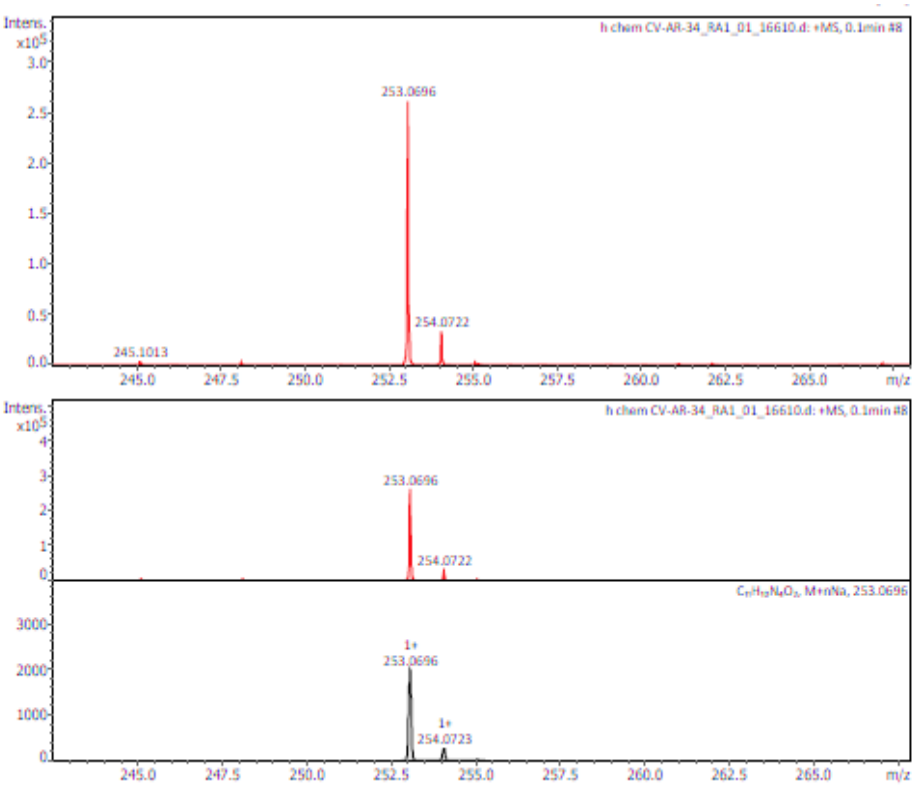

Figure 47. HR-MS of **19c** in MeOH

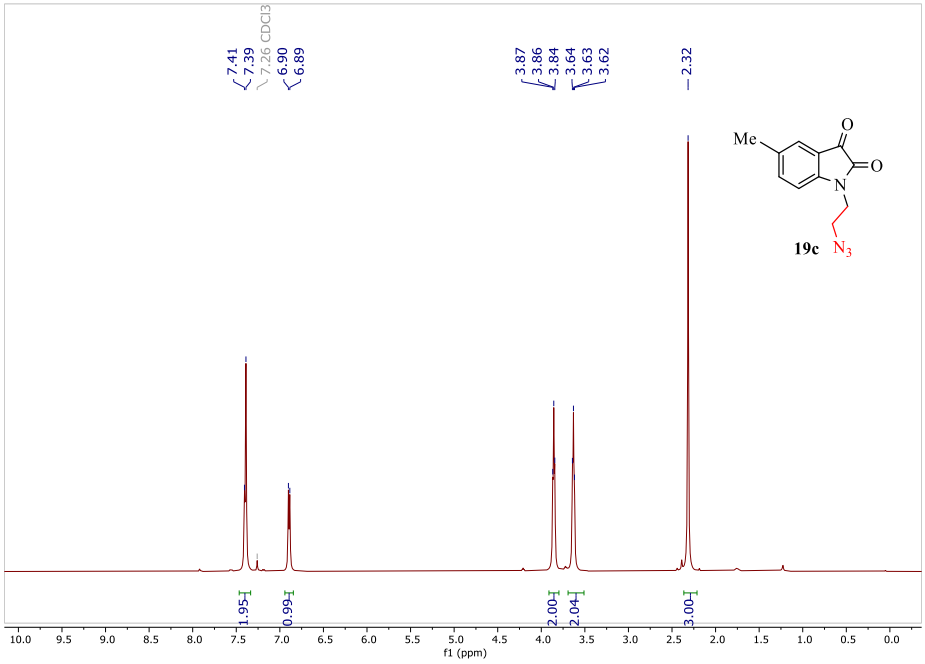

Figure 48. ^{1}H NMR spectrum of **19c** in $CDCl_3$

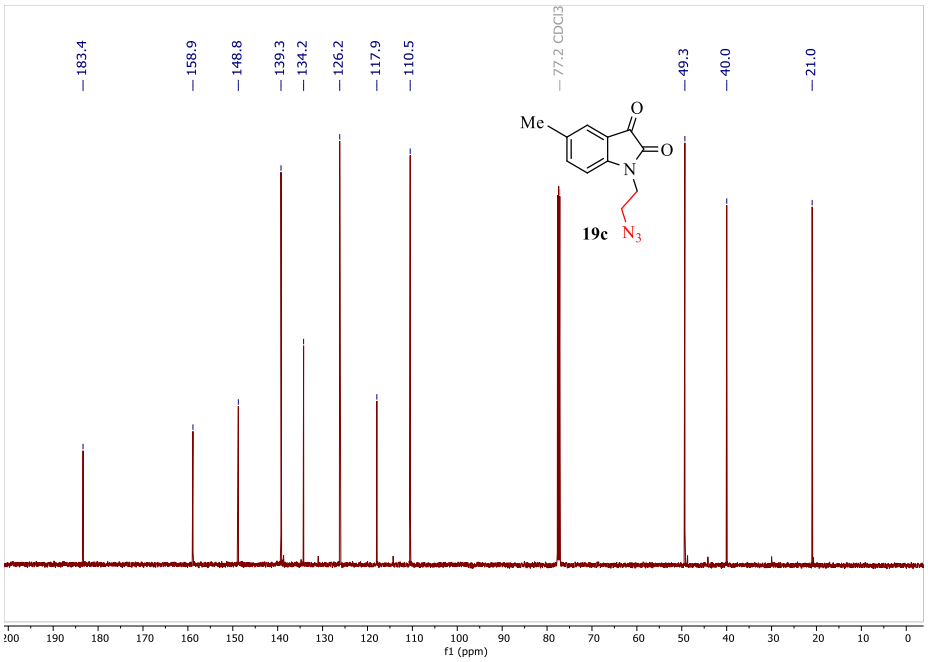

Figure 49. ^{13}C NMR spectrum of **19c** in $CDCl_3$

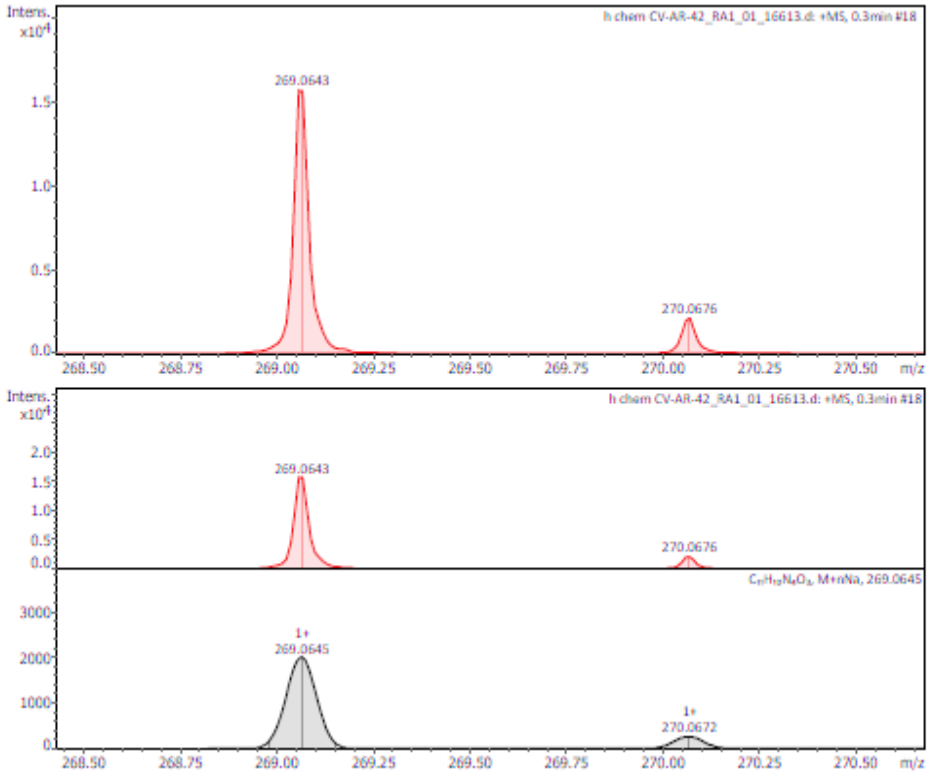

Figure 50. HR-MS of **19d** in MeOH

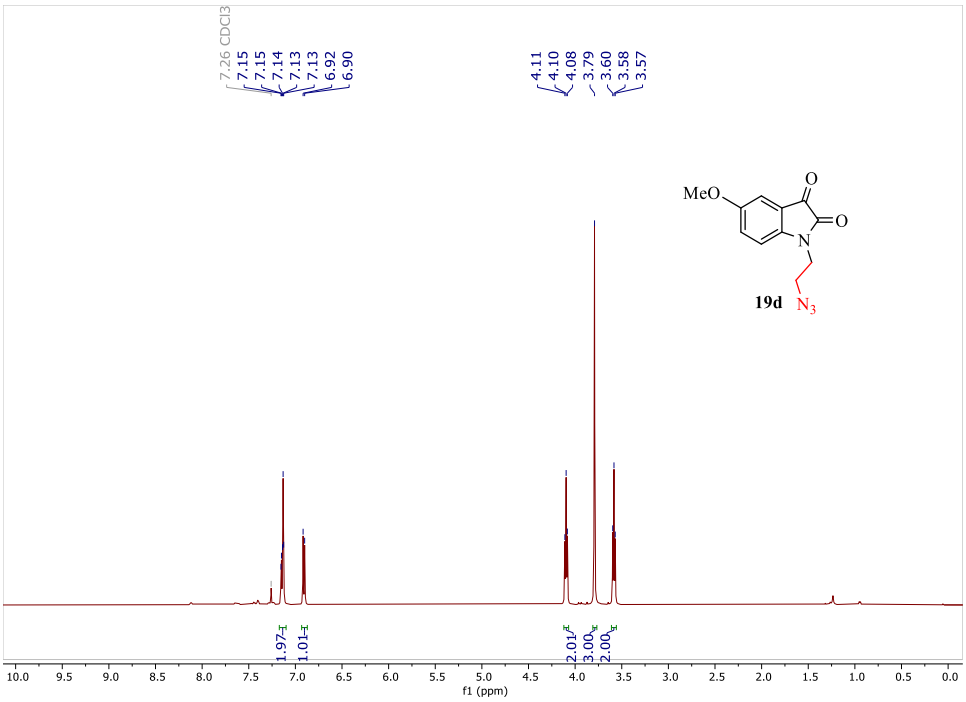

Figure 51. ^{1}H NMR spectrum of **19d** in $CDCl_3$

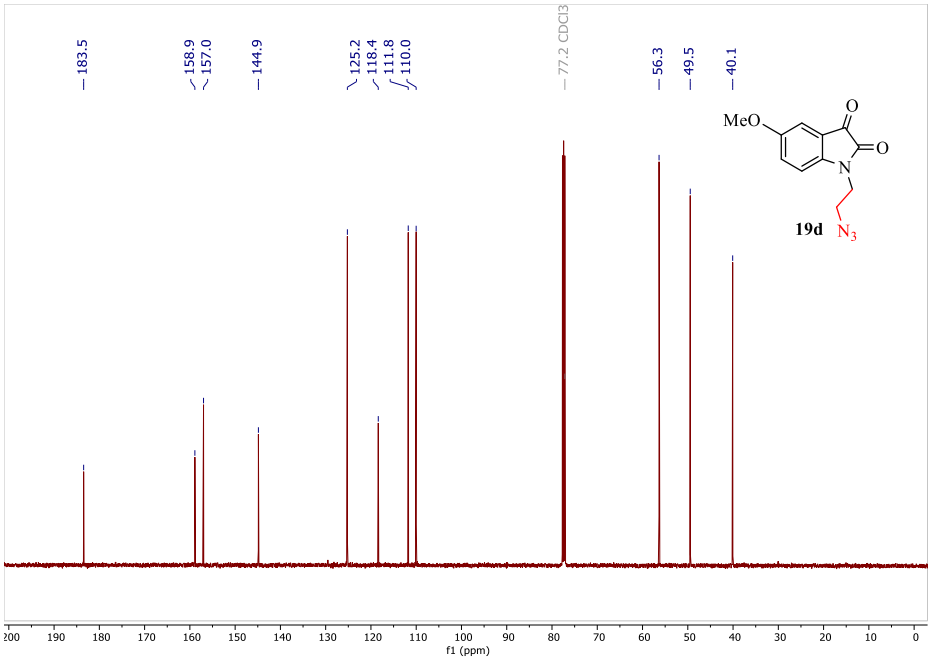

Figure 52. ^{13}C NMR spectrum of **19d** in $CDCl_3$

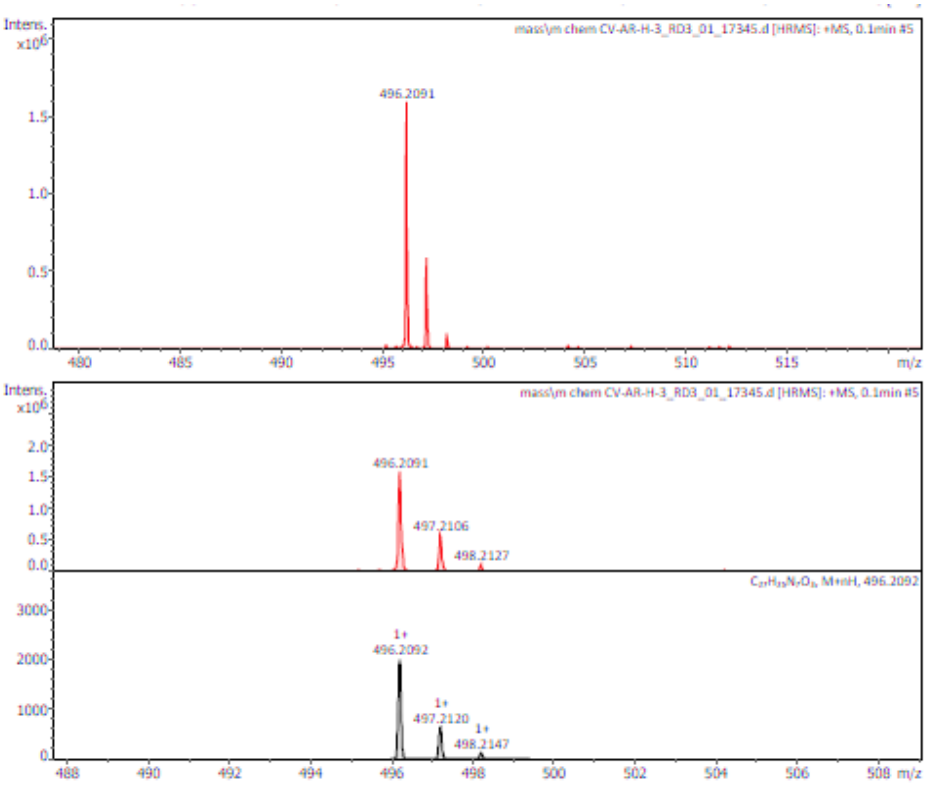

Figure 53. HR-MS of **20** in MeOH

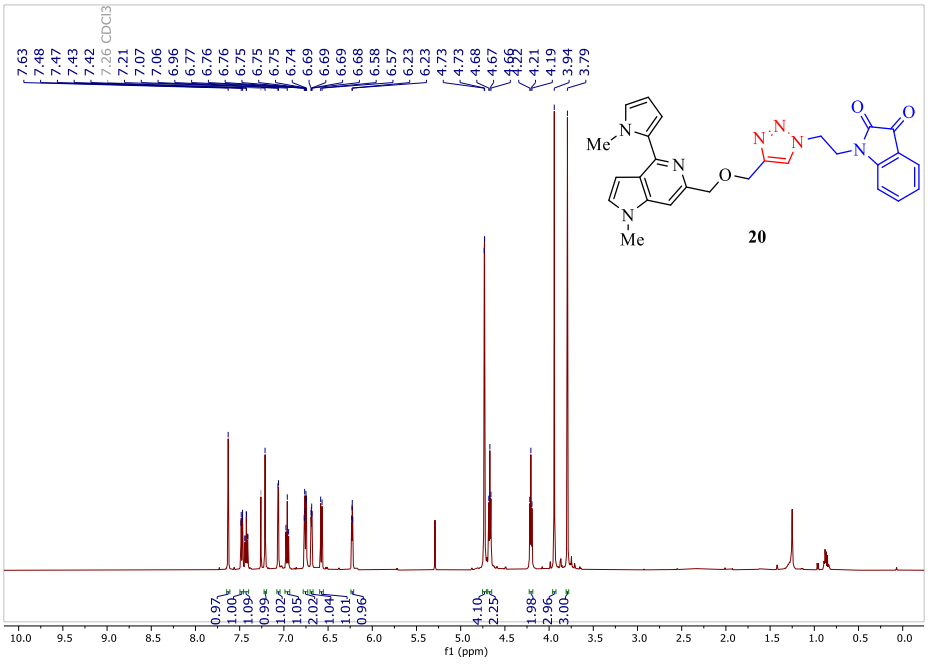

Figure 54. ^{1}H NMR spectrum of **20** in $CDCl_3$

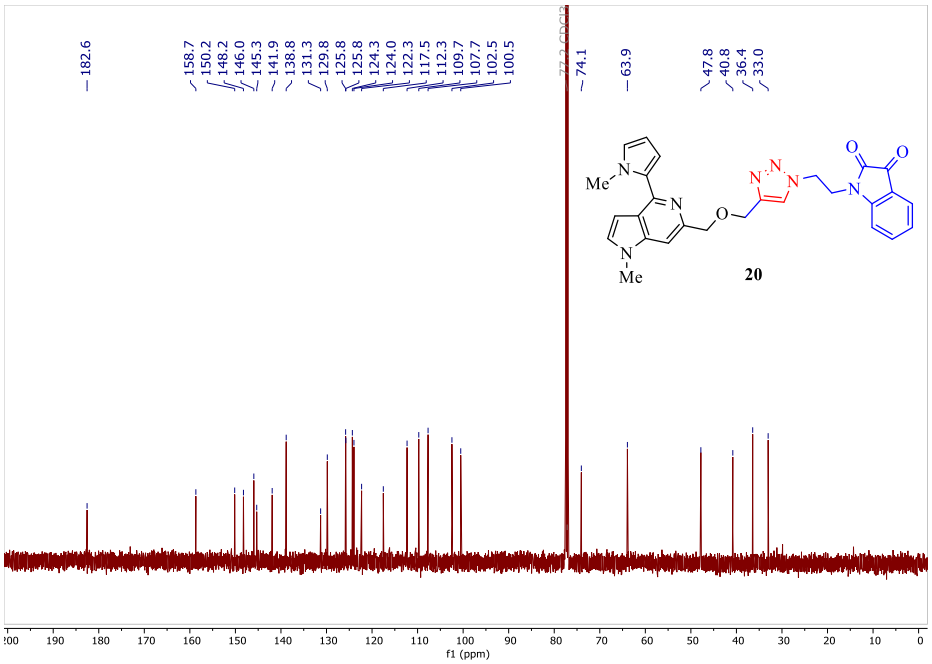

Figure 55. ^{13}C NMR spectrum of **20** in $CDCl_3$

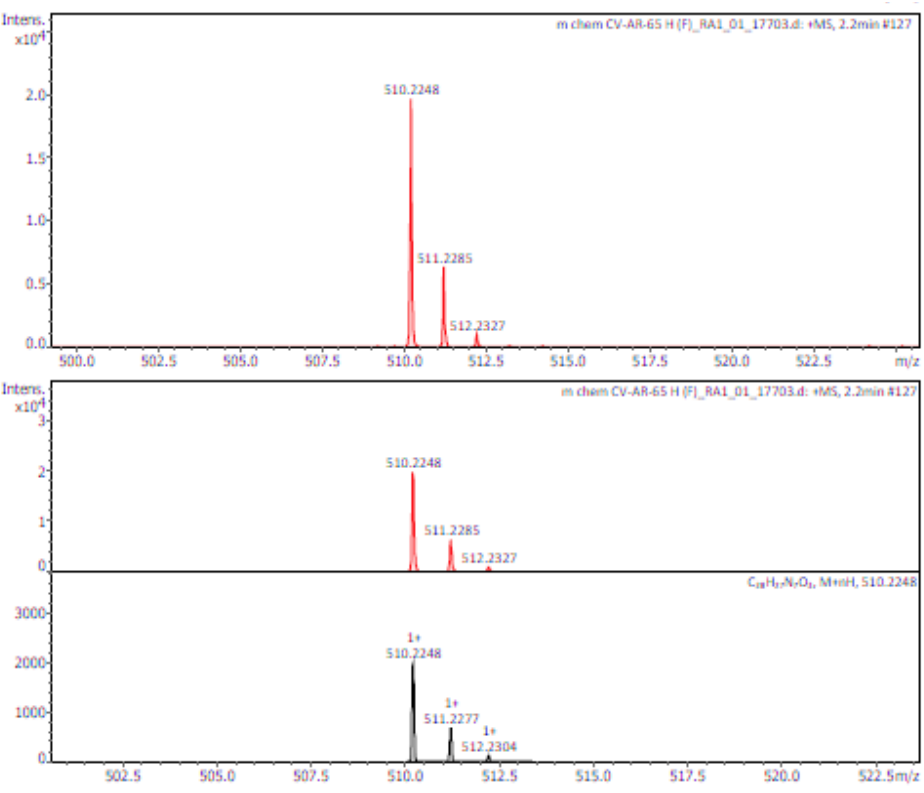

Figure 56. HRMS spectrum of **21** in MeOH

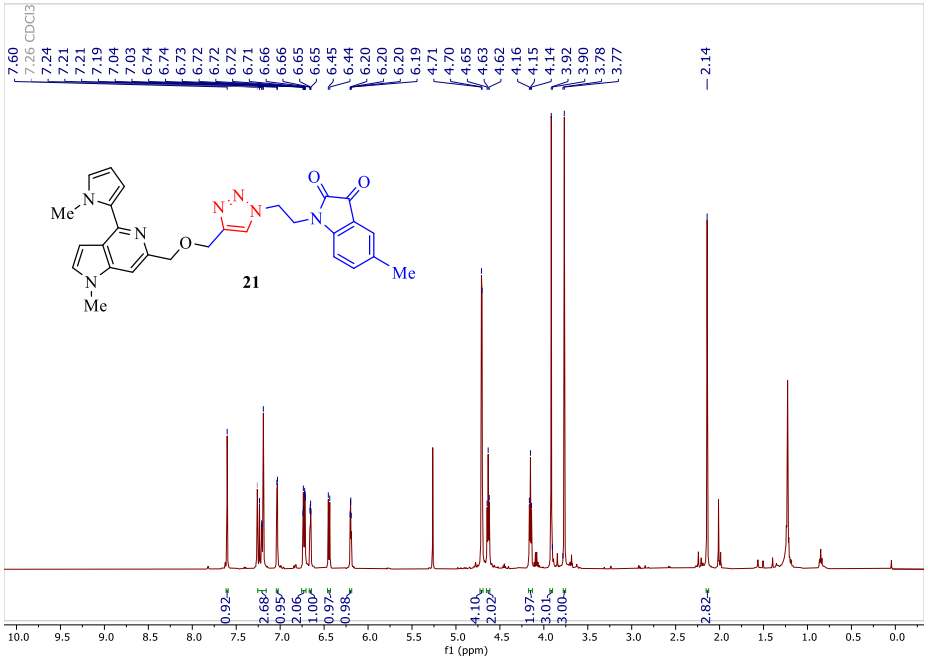

Figure 57. ^{1}H NMR spectrum of **21** in $CDCl_3$

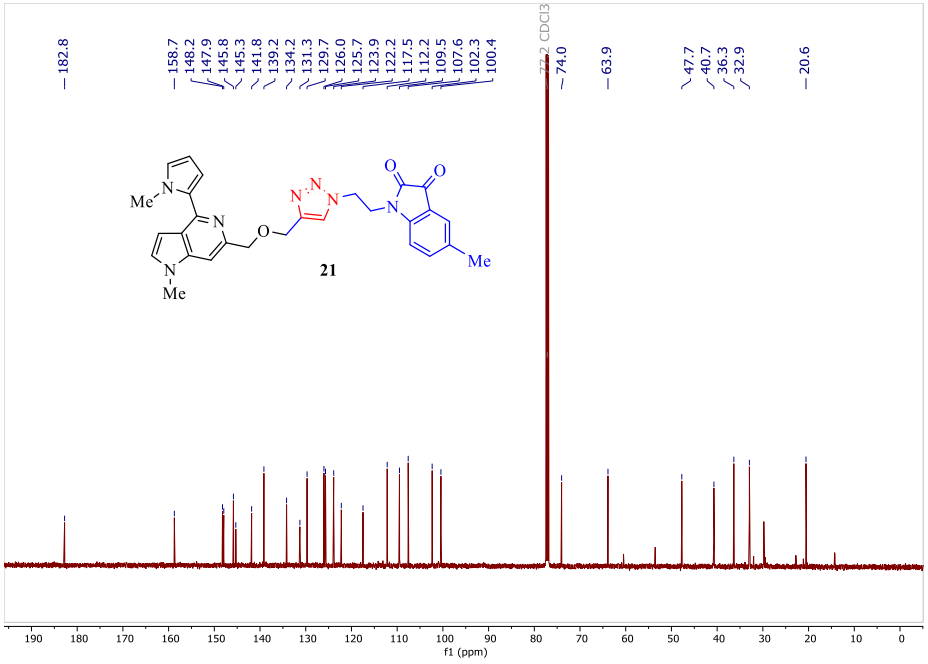

Figure 58. ^{13}C NMR spectrum of **21** in $CDCl_3$

REFERENCES

1. WHO, Global TB report, World Health Organization, Geneva, 2021.
2. Dudhe, P., Venkatasubbaiah, K., Pathak, B., & Chelvam, V. (2020). Serendipitous base-catalysed condensation–heteroannulation of iminoesters: a regioselective route to the synthesis of 4, 6-disubstituted 5-azaindoles. Organic & Biomolecular Chemistry, 18, 1582.
3. Mérour, J. Y., Buron, F., Plé, K., Bonnet, P., & Routier, S. (2014). The azaindole framework in the design of kinase inhibitors. Molecules, 19, 19935.
4. Prudhomme, M. (2003). Rebeccamycin analogues as anti-cancer agents. European Journal of Medicinal Chemistry, 38, 123.
5. Echalier, A., Bettayeb, K., Ferandin, Y., Lozach, O., Clément, M., Valette, A., Liger, F., Marquet, B., Morris, J. C., Endicott, J. A., Joseph, B., & Meijer, L. (2008). Meriolins (3-(pyrimidin-4-yl)-7-azaindoles): Synthesis, kinase inhibitory activity, cellular effects, and structure of a CDK2/cyclin A/meriolin complex. Journal of Medicinal Chemistry, 51, 737.
6. Walker, S. R., Carter, E. J., Huff, B. C., & Morris, J. C. (2009). Variolins and related alkaloids. Chemical Reviews, 109, 3080.
7. Song, J. J., Reeves, J. T., Gallou, F., Tan, Z., Yee, N. K., & Senanayake, C. H. (2007). Organometallic methods for the synthesis and functionalization of azaindoles. Chemical Society Reviews, 36, 1120.
8. Lachance, N., April, M., & Joly, M. A. (2005). Rapid and efficient microwave-assisted synthesis of 4-, 5-, 6-and 7-azaindoles. Synthesis, 15, 2571.
9. Spergel, S. H., Okoro, D. R., & Pitts, W. (2010). One-pot synthesis of azaindoles via palladium-catalyzed α-heteroarylation of ketone enolates. The Journal of Organic Chemistry, 75, 5316.

10. McLaughlin, M., Palucki, M., & Davies, I. W. (2006). Efficient access to azaindoles and indoles. Organic Letters, 8, 3307.

11. Whelligan, D. K., Thomson, D. W., Taylor, D., & Hoelder, S. (2010). Two-step synthesis of aza-and diazaindoles from chloroamino-N-heterocycles using ethoxyvinylborolane. The Journal of Organic Chemistry, 75, 11.

12. Dias Pires, M. J., Poeira, D. L., & Marques, M. M. B. (2015). Metal-catalyzed cross-coupling reactions of aminopyridines. European Journal of Organic Chemistry, 2015, 7197.

13. Mérour, J. Y., Buron, F., Plé, K., Bonnet, P., & Routier, S. (2014). The azaindole framework in the design of kinase inhibitors. Molecules, 19, 19935.

14. Zhao, S. B., & Wang, S. (2010). Luminescence and reactivity of 7-azaindole derivatives and complexes. Chemical Society Reviews, 39, 3142.

15. Prokopov, A. A., & Yakhontov, L. N. (1994). Chemistry of the azaindoles. Pharmaceutical Chemistry Journal, 28, 471.

16. Mérour, J. Y., Routier, S., Suzenet, F., & Joseph, B. (2013). Recent advances in the synthesis and properties of 4-, 5-, 6-or 7-azaindoles. Tetrahedron, 69, 4767.

17. Popowycz, F., Mérour, J. Y., & Joseph, B. (2007). Synthesis and reactivity of 4-, 5- and 6-azaindoles. Tetrahedron, 63, 8689.

18. Kennis L. E., Bischoff F. P., Mertens C. J., Love C. J., Van den Keybus F. A., Pieters Braeken M., Megens A. A., Leysen J. E. (2000). New 2-substituted 1,2,3,4-tetrahydrobenzofuro [3, 2-c] pyridine having highly active and potent central 2-antagonistic activity as potential anti-depressants. Biorganic and Medicinal Chemistry, 10, 71.

19. Fumagalli, F., de Melo, S. M. G., Ribeiro, C. M., Solcia, M. C., Pavan, F. R., Silva Emery, F. (2000). Exploiting the furo [2, 3-b] pyridine core against multidrug-resistant Mycobacterium tuberculosis. Bioorganic Medicinal Chemistry Letters, 29, 974.

20. Aggarwal A., Parai M. K., Shetty N., Wallis D., Woolhiser L., Hastings C., Dutta N. K., Galaviz S., Dhakal R.C., Shrestha R., Wakabayashi S., Walpole C., Matthews D., Floyd D., Scullion P., Riley J., Epemolu O., Norval S., Snavely T., Robertson G. T., Rubin E. J., Ioerger T. R., Sirgel F. A., van der Merwe R., van Helden P. D., Keller P., Bottger E. C., Karakousis P. C., Lenaerts A. J., Sacchettini J. C. (2017). Development of a novel lead that targets M. tuberculosis polyketide synthase 13. Cell, 170, 249.

21. Takayama, K., Wang, C., & Besra, G. S. (2005). Pathway to synthesis and processing of mycolic acids in Mycobacterium tuberculosis. Clinical Microbiology Reviews, 18, 81.

22. Vilchèze, C., & Jacobs Jr, W. R. (2014). Resistance to isoniazid and ethionamide in Mycobacterium tuberculosis: Genes, mutations, and causalities. Microbiology Spectrum, 2, 2.

23. González, A., Quirante, J., Nieto, J., Almeida, M. R., Saraiva, M. J., Planas, A., Arsequell, G., & Valencia, G. (2009). Isatin derivatives, a novel class of transthyretin fibrillogenesis inhibitors. Bioorganic & Medicinal Chemistry letters, 19, 5270.

24. Aboul-Fadl, T., Mohammed, F. A. H., & Hassan, E. A. S. (2003). Synthesis, antitubercular activity and pharmacokinetic studies of some Schiff bases derived from 1-alkylisatin and isonicotinic acid hydrazide (INH). Archives of Pharmacal Research, 26, 778.

25. Sridhar, S. K., Saravanan, M., & Ramesh, A. (2001). Synthesis and antibacterial screening of hydrazones, Schiff and Mannich bases of isatin derivatives. European Journal of Medicinal Chemistry, 36, 615.

26. Karalı, N., Gürsoy, A., Kandemirli, F., Shvets, N., Kaynak, F. B., Özbey, S., Kovalishyn, V., & Dimoglo, A. (2007). Synthesis and structure–antituberculosis activity relationship of 1H-indole-2, 3-dione derivatives. Bioorganic & Medicinal Chemistry, 15, 5888.

27. Xu, Z., Song, X. F., Hu, Y. Q., Qiang, M., & Lv, Z. S. (2017). Azide-alkyne cycloaddition towards 1H-1, 2, 3-triazole-tethered

gatifloxacin and isatin conjugates: Design, synthesis, and in vitro anti-mycobacterial evaluation. European Journal of Medicinal Chemistry, 138, 66.

28. Thomas, K. D., Adhikari, A. V., Chowdhury, I. H., Sumesh, E., & Pal, N. K. (2011). New quinolin-4-yl-1, 2, 3-triazoles carrying amides, sulphonamides and amidopiperazines as potential antitubercular agents. European Journal of Medicinal Chemistry, 46, 2503.

29. Viegas-Junior, C., Danuello, A., da Silva Bolzani, V., Barreiro, E. J., & Fraga, C. A. M. (2007). Molecular hybridization: a useful tool in the design of new drug prototypes. Current medicinal chemistry, 14, 1829.

30. Pandeya, S. N., Sriram, D., Yogeeswari, P., & Ananthan, S. (2001). Antituberculous activity of norfloxacin mannich bases with isatin derivatives. Chemotherapy, 47, 266.

31. Bhongade, B. A., Talath S., (2013). Synthesis and antibacterial evaluation of some new N-(3-chloro-4-substituted phenyl) guanidines. Indo American Journal of Pharmaceutical Research, 3,1293.

32. Aboul-Fadl, T., Bin-Jubair, F. A., & Aboul-Wafa, O. (2010). Schiff bases of indoline-2, 3-dione (isatin) derivatives and nalidixic acid carbohydrazide, synthesis, antitubercular activity and pharmacophoric model building. European Journal of Medicinal Chemistry, 45, 4578.

33. Sriram, D., Yogeeswari, P., & Meena, K. (2006). Synthesis, anti-HIV and antitubercular activities of isatin derivatives. Die Pharmazie-An International Journal of Pharmaceutical Sciences, 61, 274.

34. Feng, L. S., Liu, M. L., & Zhang, Y. B. (2012). Synthesis and *in vitro* antimycobacterial activity of moxifloxacin methylene and ethylene isatin derivatives. Chemical Research in Chinese Universities, 28, 61.

35. Xu, Z., Qiang, M., & Lv, Z. (2017). Synthesis and in vitro antimycobacterial activity of ciprofloxacin acetyl isatin derivatives. Asian Journal of Chemistry, 29, 1039.

36. Pires, M. J., Poeira, D. L., Purificacao, S. I., & Marques, M. M. B. (2016). Synthesis of substituted 4-, 5-, 6-, and 7-azaindoles from

aminopyridines via a cascade C–N cross-coupling/heck reaction. Organic letters, 18, 3250.

37. Calvet, G., Livecchi, M., & Schmidt, F. (2011). Synthesis of polysubstituted 5-azaindoles via palladium-catalyzed heteroannulation of diarylalkynes. The Journal of Organic Chemistry, 76, 4734.

38. Purificacao, S. I., Pires, M. J., Rippel, R., Santos, A. S., & Marques, M. M. B. (2017). One-pot synthesis of 1, 2-disubstituted 4-, 5-, 6-, and 7-azaindoles from amino-o-halopyridines via N-arylation/Sonogashira/cyclization reaction. Organic Letters, 19, 5118.

39. Sriram, D., Aubry, A., Yogeeswari, P., & Fisher, L. M. (2006). Gatifloxacin derivatives: synthesis, antimycobacterial activities, and inhibition of Mycobacterium tuberculosis DNA gyrase. Bioorganic & Medicinal Chemistry Letters, 16, 2982.

40. Sriram, D., Yogeeswari, P., Basha, J. S., Radha, D. R., & Nagaraja, V. (2005). Synthesis and antimycobacterial evaluation of various 7-substituted ciprofloxacin derivatives. Bioorganic & Medicinal Chemistry, 13, 5774.

41. Dighe, R.D., Rohom, S.S., Dighe, P.D., Shiradkar, M.R. (2011). Condensed bridgehead nitrogen heterocyclic systems: Synthesis and evaluation of isatinyl thiazole derivatives as anti-Mycobacterium tuberculosis agents and dTDP-rhamnose inhibitors. Der Pharma Chemica, 3, 418.

42. Eldehna, W. M., Fares, M., Abdel-Aziz, M. M., & Abdel-Aziz, H. A. (2015). Design, synthesis, and antitubercular activity of certain nicotinic acid hydrazides. Molecules, 20, 8800.

43. Gao, F., Yang, H., Lu, T., Chen, Z., Ma, L., Xu, Z., Schaffer, P., & Lu, G. (2018). Design, synthesis, and anti-mycobacterial activity evaluation of benzofuran-isatin hybrids. European Journal of Medicinal Chemistry, 159, 277.